The Plant Cell, Vol. 16, 3002–3019, November 2004, www.plantcell.org © 2004 American Society of Plant Biologists

Novel Targeting Signals Mediate the Sorting of Different Isoforms of the Tail-Anchored Membrane Protein Cytochrome b_5 to Either Endoplasmic Reticulum or Mitochondria

Yeen Ting Hwang,[a] Scott M. Pelitire,[b] Matthew P.A. Henderson,[c] David W. Andrews,[c] John M. Dyer,[b,1] and Robert T. Mullen[a,1,2]

[a] Department of Botany, University of Guelph, Guelph, Ontario N1G 2W1, Canada
[b] U.S. Department of Agriculture, Agricultural Research Service, Southern Regional Research Center, New Orleans, Louisiana 70124
[c] Department of Biochemistry, McMaster University, Hamilton, Ontario L8N 3Z5, Canada

Tail-anchored membrane proteins are a class of proteins that are targeted posttranslationally to various organelles and integrated by a single segment of hydrophobic amino acids located near the C terminus. Although the localization of tail-anchored proteins in specific subcellular compartments in plant cells is essential for their biological function, the molecular targeting signals responsible for sorting these proteins are not well defined. Here, we describe the biogenesis of four closely related tung (*Aleurites fordii*) cytochrome b_5 isoforms (Cb5-A, -B, -C, and -D), which are small tail-anchored proteins that play an essential role in many cellular processes, including lipid biosynthesis. Using a combination of in vivo and in vitro assays, we show that Cb5-A, -B, and -C are targeted exclusively to the endoplasmic reticulum (ER), whereas Cb5-D is targeted specifically to mitochondrial outer membranes. Comprehensive mutational analyses of ER and mitochondrial Cb5s revealed that their C termini, including transmembrane domains (TMD) and tail regions, contained several unique physicochemical and sequence-specific characteristics that defined organelle-specific targeting motifs. Mitochondrial targeting of Cb5 was mediated by a combination of hydrophilic amino acids along one face of the TMD, an enrichment of branched β-carbon–containing residues in the medial portion of the TMD, and a dibasic -R-R/K/H-x motif in the C-terminal tail. By contrast, ER targeting of Cb5 depended primarily upon the overall length and hydrophobicity of the TMD, although an -R/H-x-Y/F- motif in the tail was also a targeting determinant. Collectively, the results presented provide significant insight into the early biogenetic events required for entry of tail-anchored proteins into either the ER or mitochondrial targeting pathways.

INTRODUCTION

Tail-anchored (TA) membrane proteins are a functionally diverse group of proteins that are found on nearly all cellular membranes and share several distinct structural features, including an N-terminal cytosolic domain that represents the majority of the protein, a single hydrophobic segment located near the C terminus, and a short C-terminal tail sequence that protrudes into the organelle lumen (Kutay et al., 1993). Although the orientation of TA proteins ($N_{cytosol}$-C_{lumen}) is similar to that of classical type II membrane proteins ($N_{cytosol}$-C_{lumen}), the two groups of proteins are targeted and inserted into membranes in different ways. Type II membrane proteins are sorted during translation by the signal recognition particle (SRP)/Sec61p pathway to the endoplasmic reticulum (ER) exclusively, whereas TA proteins are targeted in a posttranslational (SRP-independent) manner to a variety of organelles, including ER, peroxisomes, mitochondria, and chloroplasts. Examples of TA proteins in plant cells include peroxisomal ascorbate peroxidase (Bunkelmann and Trelease, 1996), Toc34, the 34-kD polypeptide of the translocase in the outer chloroplast envelope membrane (Seedorf et al., 1995), cytochrome b_5 (Cb5), which is located in ER membranes (Smith et al., 1994), and the soluble *N*-ethylmaleidmide–sensitive factor attachment protein receptors (SNAREs), which are found in many different compartments of the endomembrane system (Sanderfoot et al., 2000). The proper localization of these and other TA proteins to their specific subcellular compartments is essential for their biochemical function. For instance, SNARE proteins play a critical role in the vectorial transport of vesicles through the secretory system, and loss of SNARE function can negatively affect many different physiological processes, including gravitropism, tissue differentiation, auxin transport, cytokinesis, stress response, and/or pathogen resistance (Pratelli et al., 2004; Surpin and Raikhel, 2004).

Although the targeting signals and pathways responsible for the localization of TA proteins in plant cells have not been defined (with the exception of peroxisomal ascorbate peroxidase; Mullen

[1] These authors contributed equally to this work.
[2] To whom correspondence should be addressed. E-mail rtmullen@uoguelph.ca; fax 519-767-1991.
The author responsible for distribution of materials integral to the findings presented in this article in accordance with the policy described in the Instructions for Authors (www.plantcell.org) is: Robert T. Mullen (rtmullen@uoguelph.ca).
Article, publication date, and citation information can be found at www.plantcell.org/cgi/doi/10.1105/tpc.104.026039.

et al., 1999; Mullen and Trelease, 2000), details regarding the biogenesis of mammalian and yeast TA proteins are relatively well characterized (reviewed in Wattenberg and Lithgow, 2001; Borgese et al., 2003). The targeting signals present in mammalian and yeast TA proteins are located within their C termini, and because this region of the proteins does not exit the ribosome until translation is complete, TA proteins must engage their respective organelle-specific targeting pathways in a posttranslational manner. The majority of nascent TA proteins are initially sorted from the cytosol to either the ER or mitochondrial outer membrane by independent but competing pathways (Borgese et al., 2001, 2003), and many of the ER-targeted TA proteins are subsequently transported to other compartments of the endomembrane system (e.g., Golgi, vacuole, plasma membrane, etc.). It is now well established that the C-terminal targeting signals that mediate the initial posttranslational sorting of mammalian and yeast TA proteins to the ER or mitochondria are not contained within specific amino acid sequences, but rather consist of general physicochemical properties of the transmembrane domain (TMD) and tail sequences (Isenmann et al., 1998; Kuroda et al., 1998; Borgese et al., 2001; Pedrazzini et al., 2001; Horie et al., 2002, 2003; Beilharz et al., 2003; Kaufmann et al., 2003). For example, mitochondrial targeting of mammalian TA proteins generally requires a shorter TMD (<20 residues) sequence and a tail region that is enriched in positively charged amino acids, whereas ER targeting requires a longer TMD with fewer positively charged residues in the tail sequence. Although these similarities in the targeting signals allow some TA proteins to exhibit dual localization within the cell, most TA proteins are targeted exclusively to one organelle or the other (Borgese et al., 2003). Notably, only mammalian cells have been shown to contain two distinct isoforms of Cb5 that are localized specifically to the ER or to the mitochondrial outer membrane (Ito, 1980; Lederer et al., 1983; D'Arrigo et al., 1993). Despite intensive efforts over the past few years, details related to the nature of the cellular machinery involved in targeting and membrane integration of TA proteins to either ER or mitochondrial membranes in any organism have not been resolved (reviewed in Borgese et al., 2003; for an alternate point of view, see Abell et al., 2004).

To begin to characterize the molecular mechanisms involved in the biogenesis of TA proteins in plant cells, we have identified and characterized four different isoforms of Cb5 from developing tung (*Aleurites fordii* Hemsl.) seeds. Tung is a subtropical tree that produces a seed oil containing high amounts of eleostearic acid (18:3$\Delta^{9cis,11trans,13trans}$), an unusual conjugated fatty acid that imparts industrially useful drying qualities to the oil (Sonntag, 1979). We previously identified the enzyme required for eleostearic acid biosynthesis, a diverged, Cb5-dependent Δ^{12} oleic acid desaturase (FAD2) termed FADX (Dyer et al., 2002), and subsequently determined the mechanisms for FAD targeting and assembly into ER membranes in plant cells (McCartney et al., 2004). Here, we report the identification, functional analysis, and a detailed description of the molecular targeting signals for four Cb5 proteins that are expressed in developing tung seeds during biosynthesis of tung oil. We show that three of the isoforms (Cb5-A, -B, and -C) are localized exclusively to the ER of plant cells, whereas the fourth isoform (Cb5-D) is targeted specifically to the outer membrane of plant mitochondria. Interestingly, similar targeting results were obtained in vitro with ER and mitochondrial membranes derived from mammalian cells, suggesting that at least some aspects of Cb5 biogenesis are conserved among plants and mammals. We demonstrate also, using extensive mutagenic analysis, that plant Cb5s contain novel, discrete targeting signal motifs in addition to general physicochemical characteristics that confer higher fidelity sorting to ER or mitochondria in comparison with their mammalian Cb5 counterparts. Overall, the results indicate that the targeting signals responsible for sorting Cb5 isoforms to different organelles in plant cells are highly complex and include several novel features that have not been proposed to be involved in the sorting of TA proteins in other eukaryotic cells.

RESULTS

Sequence Features, Gene Expression Patterns, and Functionality of Four Tung Cb5 Isoforms

Four unique cDNAs, each encoding a putative Cb5 protein designated as either Cb5-A, -B, -C, or -D were isolated from a developing tung seed cDNA library. Comparisons of the deduced amino acid sequences of the four polypeptides revealed that they each exhibited conserved features of the Cb5 protein family, including a heme binding motif (-HPGG-) and a single putative TMD located near the C terminus (Figure 1A). Isoforms A, B, and C were the most similar overall, sharing 65 to 79% amino acid sequence identity, whereas Cb5-D shared only ~40% identity with the other three isoforms. Phylogenetic analysis indicated that Cb5-B and Cb5-C likely have a paralogous relationship because of a relatively recent gene duplication event (Figure 1B) and that Cb5-D is the most diverged isoform located in a deeply branched clade that is well separated from the other three tung Cb5 proteins. Whereas all four tung Cb5 isoforms were initially identified in a developing seed cDNA library, genes encoding Cb5-B and Cb5-C were expressed at higher levels in leaves, Cb5-A was expressed mostly in seeds, and Cb5-D was difficult to detect in either leaves or seeds (Figure 1C).

To assess the functional properties of the four tung Cb5 proteins, each isoform was expressed individually in yeast cells that harbored a disruption in the single endogenous Cb5 gene (*CYB5*) but contained an ectopically expressed, Cb5-dependent FAD2 from tung (Dyer et al., 2002). Control experiments revealed that FAD2 activity was substantially reduced in mutant cells lacking the endogenous Cb5 protein, as judged by a decrease in the amount of linoleic acid produced by FAD2 in Δ*CYB5* cells in comparison with the amount produced by FAD2 in wild-type cells (Figure 1D). The residual FAD2 activity detected in Δ*CYB5* cells lacking a coexpressed tung Cb5 was most likely because of interaction of FAD2 with the Cb5 domain of endogenous stearoyl-CoA desaturase (Petrini et al., 2004). Figure 1D shows also that coexpression of any of the four tung Cb5 proteins with FAD2 in the mutant Δ*CYB5* strain fully restored FAD2 activity, demonstrating that each Cb5 protein could functionally complement yeast Cb5 activity. Similar complementation results were obtained when using N-terminally myc-tagged Cb5 proteins or when each Cb5 protein was coexpressed in Δ*CYB5* cells with

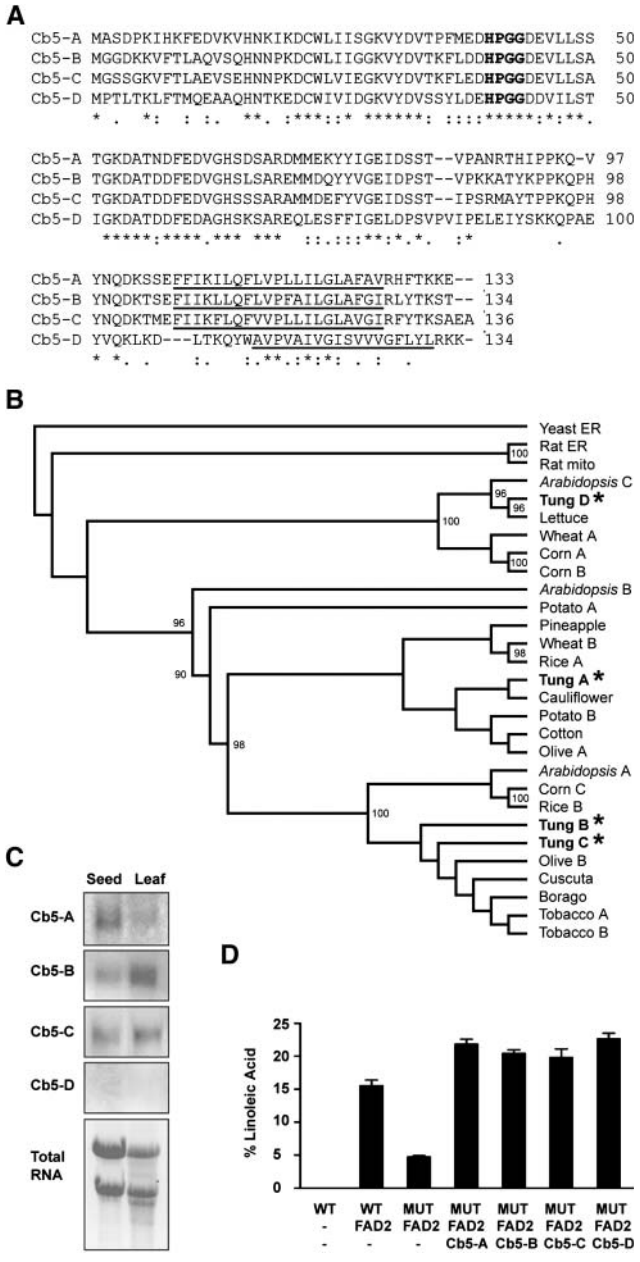

Figure 1. Comparison of Tung Cb5-A, -B, -C, and -D Polypeptide Sequences, Phylogentic Relationships, Gene Expression Patterns, and Functional Analysis.

(A) Deduced amino acid sequence alignment of tung Cb5 isoforms showing the presence of conserved features of the Cb5 protein family, including predicted heme binding domains (bold) and C-terminal TMDs (underlined). Identical residues in each of the aligned Cb5 isoforms are indicated by asterisks, highly similar residues are indicated with colons, and similar residues are indicated by dots. Sequences were aligned using the ClustalW algorithm, and TMDs were identified using TMHMM (version 2.0).

(B) Phylogenetic relationships of various Cb5 proteins. Phylogenetic analysis of Cb5 protein sequences was performed using the ClustalX windows interface (version 1.8), and the resulting phylogram was plotted with TreeView (version 1.6.6). The tree was rooted with yeast Cb5, and bootstrap values (from 1000 iterations) above 90% are shown at each node. Tung Cb5 isoforms are in bold and marked with an asterisk.

(C) RNA gel blot analysis of the expression of Cb5 genes in either tung seeds or leaves. Membranes were hybridized with dig-labeled riboprobes derived from full-length sequences encoding each Cb5 isoform, and blots were developed using chemiluminescent substrates. Ethidium bromide–stained total RNA is shown as a loading control.

(D) Functional complementation of yeast Cb5 protein activity. Wild-type or mutant (MUT; lacking the endogenous *CYB5* gene) yeast cells were either transformed with FAD2 (a Cb5-dependent desaturase that produces linoleic acid from endogenous oleic acid; Dyer et al., 2002) or cotransformed with FAD2 and either tung Cb5-A, -B, -C, or -D. Strain and plasmid combinations are shown along the *x* axis. Cells were grown overnight in galactose-containing medium and then harvested, lipids were extracted, and fatty acid composition determined by gas chromatography and flame ionization detection using methyl heptadecanoate as an internal standard. Content of linoleic acid (% wt/wt total fatty acid methylesters) in yeast lipids is shown along the *y* axis. Values represent the average and standard deviation of three independent experiments.

a different Cb5-dependent FAD, including tung FADX (Dyer et al., 2002) (data not shown).

Cb5-A, -B, and -C Are Localized to ER, whereas Cb5-D Is Localized to Mitochondria

To determine the subcellular localization of Cb5 isoforms A, B, C, and D, each protein was myc-epitope-tagged at its N terminus and expressed transiently in tobacco BY-2 suspension cells followed by immunofluorescence microscopic analysis. As shown in Figures 2A to 2F, myc-tagged Cb5-A, -B, and -C colocalized with endogenous calreticulin in the ER of transformed BY-2 cells. By contrast, expressed myc-tagged Cb5-D localized to punctate subcellular structures that contained endogenous E1β, a protein subunit of the pyruvate dehydrogenase complex located in the mitochondrial matrix (Luethy et al., 1995) (Figures 2G and 2H). High magnification confocal laser-scanning microscopy (CLSM) revealed that the fluorescence pattern attributable to Cb5-D was actually toroidal in shape (Figure 2I) and that these structures enclosed the spherical fluorescent structures attributable to endogenous E1β (Figures 2J and 2K). Coexpression of Cb5-D and green fluorescent protein (GFP)-Tom22 (a fusion protein consisting of GFP and the *Arabidopsis thaliana* 22-kD subunit of the translocase of the outer mitochondrial membrane; Werhahn et al., 2001) resulted in colocalization of these proteins in the same torus structures (Figures 2L to 2N), indicating that Cb5-D was localized specifically to the outer membrane of mitochondria. Additional CLSM experiments revealed that the reticular fluorescence patterns attributable to ER-localized Cb5-A, -B, and -C did not colocalize with, nor enclose, the spherical fluorescent structures attributable to E1β in the mitochondrial matrix (data shown only for myc-Cb5-A; Figures 2O to 2Q). Similarly, the toroidal fluorescence pattern attributable to expressed Cb5-D in the mitochondrial outer membrane did not overlap with the reticular fluorescence staining of calreticulin in the ER (data not shown). Collectively, these data indicate that Cb5-A, -B, and -C are sorted to the ER and that Cb5-D is sorted exclusively to the mitochondrial outer membrane.

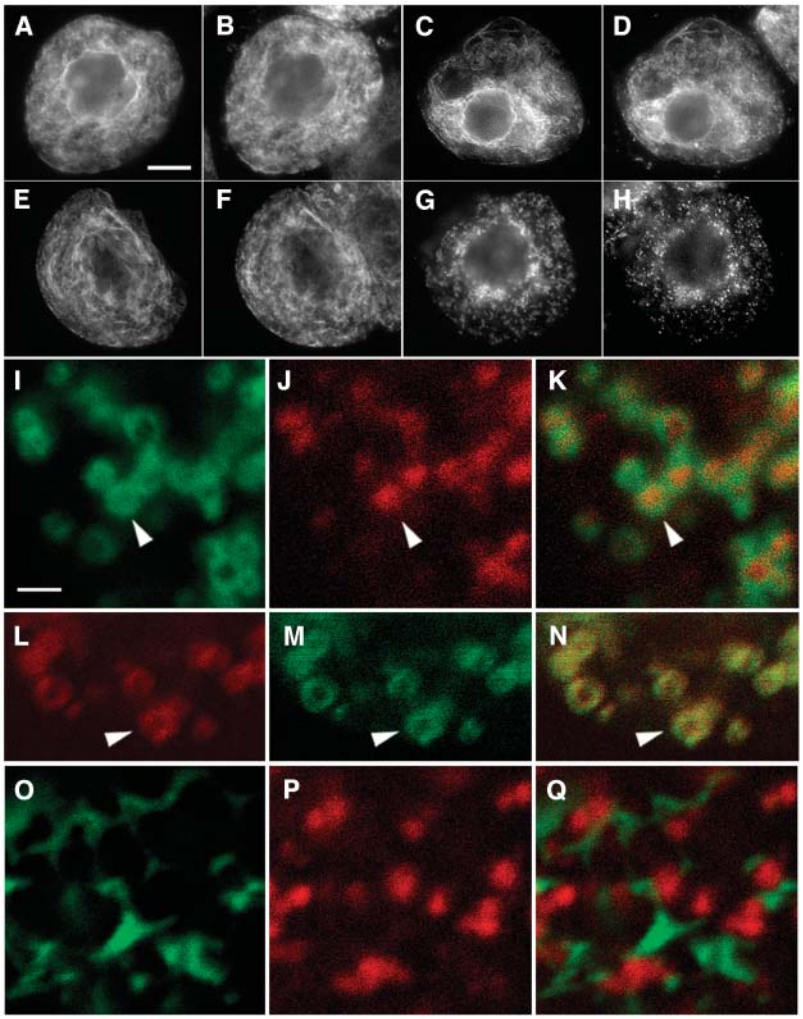

Figure 2. Subcellular Localization of Tung Cb5 Isoforms in Tobacco BY-2 Cells.

BY-2 cells were either transiently transformed (**[A]** to **[K]** and **[O]** to **[Q]**) or transiently cotransformed (**[L]** to **[N]**) with myc-tagged Cb5-D and GFP-Tom22. Fixed and (immuno)stained cells were visualized using either epifluorescence microscopy (**[A]** to **[H]**) or CLSM (**[I]** to **[Q]**). Single optical sections (~2 μm in thickness) of BY-2 cells shown in **(I)** to **(Q)** were acquired as part of a z-series. Bars = 10 μm in **(A)** and 1 μm in **(I)**.

(A) to **(F)** Transiently expressed Cb5-A **(A)**, Cb5-B **(C)**, Cb5-C **(E)**, and endogenous ER calreticulin **(B)**, **(D)**, and **(F)** in transformed cells. Note the presence of calreticulin staining in adjacent untransformed cells (**[B]**, **[D]**, and **[F]**).

(G) and **(H)** Expressed Cb5-D **(G)** and endogenous mitochondrial E1β **(H)** in a BY-2 cell.

(I) to **(K)** Expressed Cb5-D **(I)** and endogenous E1β **(J)** in a portion of a transformed BY-2 cell. The merged image of **(I)** and **(J)** in **(K)** shows that the torus fluorescent structures containing Cb5-D delineate the spherical structures attributable to mitochondrial matrix-localized E1β. Arrowheads indicate an obvious example of toroidal enclosure of a sphere.

(L) to **(N)** Coexpressed Cb5-D **(L)** and GFP-Tom22 **(M)** in a portion of a transformed BY-2 cell. The yellow color in the merged image of **(L)** and **(M)** in **(N)** indicates that Cb5-D and GFP-Tom22 are located in the same sites within the cell, presumably the mitochondrial outer membrane. Arrowheads indicate obvious colocalizations.

(O) to **(Q)** Expressed Cb5-A **(O)** and endogenous mitochondrial E1β **(P)** in a portion of a BY-2 cell. The merged image of **(O)** and **(P)** in **(Q)** demonstrates that Cb5-A does not localize with the E1β in the mitochondrial matrix.

In Vitro Insertion of Cb5 Proteins into ER and Mitochondrial Membranes

The mechanisms for tung Cb5 targeting and assembly into membranes were investigated further by incubating in vitro synthesized, radiolabeled Cb5-A or Cb5-D with ER microsomes and/or mitochondria. Figure 3A (lanes 1 to 3, + mbs) shows that Cb5-A and Cb5-D, as well as the control ER TA proteins rat Cb5 (Janiak et al., 1994a; Kim et al., 1997) and rat vesicle-associated membrane protein 2 (Vamp2) (Kim et al., 1999), bound ER membranes in a posttranslational manner, as evidenced by their recovery in bottom fractions of step gradients after centrifugation. By contrast, only a small amount of each of these proteins

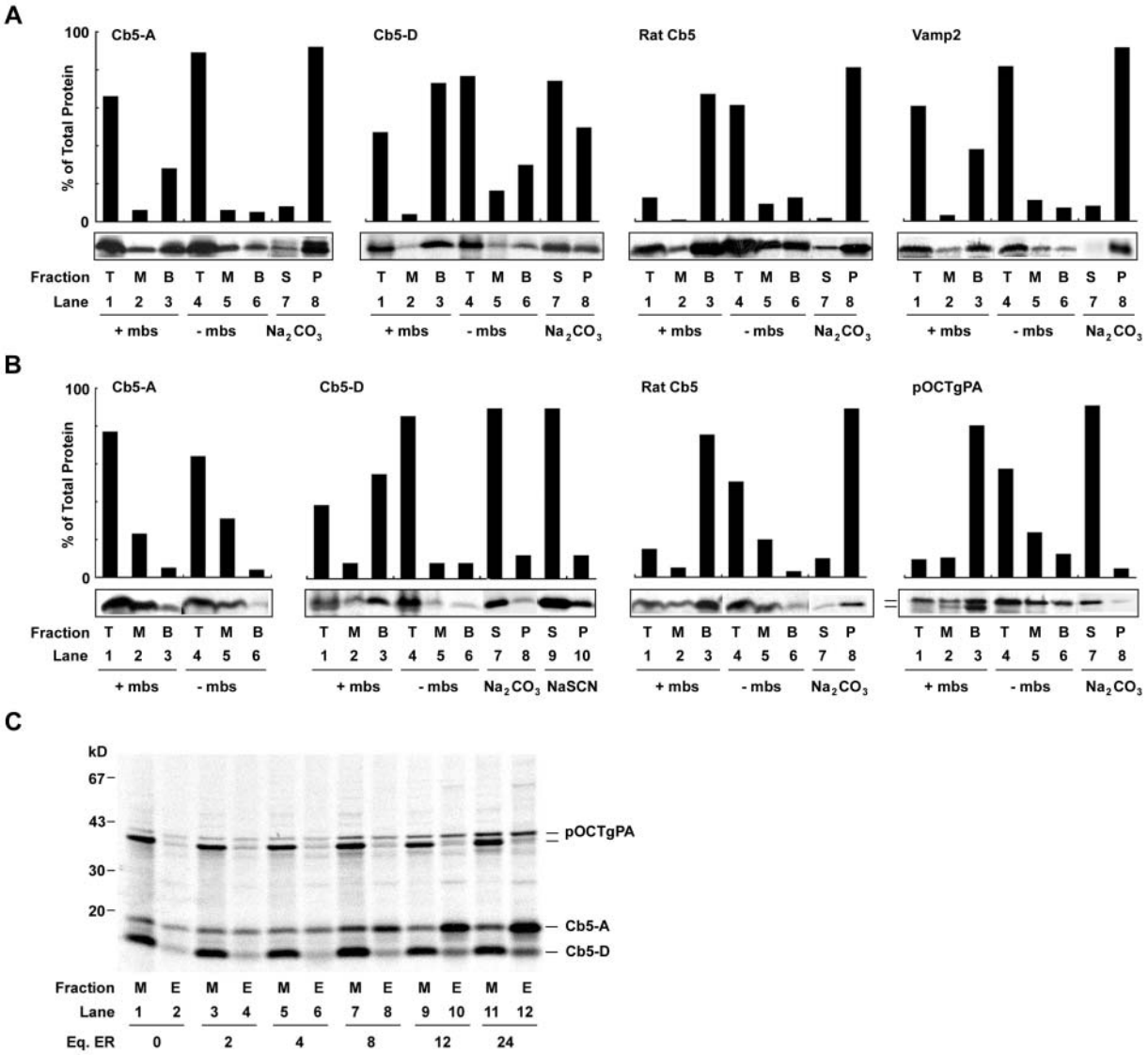

Figure 3. Targeting of Tung Cb5 Isoforms A and D to ER and/or Mitochondrial Membranes in Vitro.

(A) Targeting of various Cb5 isoforms and Vamp2 to ER membranes. Plasmids containing sequences coding for either Cb5-A, Cb5-D, rat Cb5, or rat Vamp2 were transcribed in vitro using SP6 polymerase, and transcription products were translated in reticulocyte lysate or, for Cb5-D, fractionated reticulocyte lysate (see Methods) with ^{35}S-Met. Translation products were then treated as follows: + mbs, purified pig microsomes were added after translation reactions were completed (lanes 1 to 3); or − mbs, no microsomes were added to the translation reaction (lanes 4 to 6). All reactions were layered on top of a sucrose cushion, and the microsomes were pelleted by centrifugation. The resulting gradients were divided into top (T) and middle (M) fractions containing soluble proteins and the bottom (B) fraction containing microsomes and microsomal-bound proteins. For membrane integration assays, microsome-bound proteins (bottom fractions from in vitro translation assay; + mbs lane 3) were incubated with Na_2CO_3, pH 11.5, and lumenal/peripheral proteins (S; lane 7) were separated from integral membrane proteins (P; lane 8) by centrifugation. Equivalent amounts of all fractions were analyzed by SDS-PAGE, and the percentage of the total protein recovered from each fraction was determined using a phosphor imager.

(B) Targeting of various Cb5 isoforms and pOCTgPA to mitochondria. Plasmids containing sequences coding for either Cb5-A, Cb5-D, rat Cb5, or pOCTgPA were transcribed and translated as described in **(A)**. Translation products were then treated as follows: + mbs, purified rat liver mitochondria were added after translation reactions were completed (lanes 1 to 3); or − mbs, no mitochondria were added to the translation reaction (lanes 4 to 6). Top (T), middle (M), and bottom (B) fractions collected from step gradients were analyzed using SDS-PAGE and a phosphor imager as described in **(A)**. For membrane integration assays, mitochondrial-bound proteins (bottom fractions from in vitro translation assay; + mbs lane 3) were incubated with either Na_2CO_3, pH 11.5, or NaSCN (as indicated) and then lumenal/peripheral (S; lanes 7 and 9) and integral (P; lanes 8 and 10) membrane proteins were separated by centrifugation. Equivalent amounts of all fractions were analyzed by SDS-PAGE, and the percentage of the total protein recovered from each fraction was determined using a phosphor imager. Bars in **(B)** and **(C)** indicate the migration of higher molecular weight unprocessed (full-length) pOCTgPA and lower molecular weight processed (presequence cleaved after import) OCTgPA.

sedimented in bottom fractions when pelleting assays were performed in the absence of membranes (lanes 4 to 6, − mbs), indicating that their distribution in step gradients was not because of misfolding and/or aggregation in vitro. Extraction of resuspended membranes from bottom fractions (lane 3) with 0.1 M sodium carbonate, pH 11.5, revealed that the majority (>80%) of membrane-bound Cb5-A, rat Cb5, and Vamp2 was integrated into ER membranes (lanes 7 and 8, Na_2CO_3).

Reactions with purified mitochondria (Figure 3B) revealed that a significant proportion (50%) of Cb5-D protein pelleted with mitochondria in the bottom fraction (lane 3, + mbs). By contrast, only a small amount (5%) of Cb5-A was recovered with mitochondria. The lack of Cb5-A targeting to mitochondria in vitro was surprising because other Cb5 proteins, including the ER-specific rat Cb5 used as a control (Figure 3B, lane 3, + mbs), are known to insert spontaneously into mitochondria and other membrane systems, including liposomes, in vitro (Remacle, 1978; Enoch et al., 1979; Kim et al., 1997). A soluble rat preornithine carbamyl transferase-Protein A fusion (pOCTgPA), which is known to be translocated into the mitochondrial matrix (Janiak et al., 1994a), was efficiently (84%) incorporated into mitochondria, as evidenced by processing of the presequence (cleavage) resulting in the formation of a lower molecular mass polypeptide (lane 3, + mbs). Integration assays revealed that the majority (90%) of the rat Cb5 control protein was recovered in the sodium carbonate–washed mitochondrial pellet, as expected. By contrast, Cb5-D, similar to the soluble control protein pOCTgPA, was almost completely released from mitochondria upon treatment with sodium carbonate (lanes 7 and 8, Na_2CO_3). The majority (88%) of Cb5-D was also released into the supernatant fraction when mitochondria were washed with 1 M sodium thiocyanate (lanes 9 and 10, NaSCN), but the protein was only partially released (53%) when mitochondria were washed with 1 M NaCl (data not shown). These data indicate that Cb5-D is peripherally bound to mitochondria via mostly hydrophobic rather than hydrophilic or electrostatic interactions, similar to the association of a loose binding form of mammalian Cb5 ER reported previously (Takagaki et al., 1983a, 1983b).

Although the targeting of Cb5-A to ER and not to mitochondria in vitro was consistent with our in vivo targeting data (Figure 2), the apparent indiscriminant association of Cb5-D with both membranes in vitro was somewhat unexpected given its fidelity for mitochondrial targeting in vivo. These differences may simply reflect a peculiarity of the mechanism of membrane targeting of Cb5-D or may be because of a limitation of the cell-free system, such as Cb5-D targeting to ER microsomes only as a default because of the lack of functional mitochondrial target membranes. To assess the latter possibility, we analyzed the targeting of Cb5-A and Cb5-D, along with the control protein pOCTgPA, in the same reaction containing a fixed amount of mitochondria along with varying amounts of ER membranes (Figure 3C). Consistent with the results presented above (Figure 3B) as well as those reported previously by Janiak et al. (1994b), the majority of pOCTgPA targeted to mitochondria regardless of the relative amount of ER membranes present in the reaction. These results not only confirm the targeting fidelity of the pOCTgPA control protein but indicate also that ER and mitochondria were effectively separated by differential centrifugation. Our direct competition assay confirmed also that Cb5-A displayed a high degree of specificity for ER membranes, (i.e., Cb5-A ER targeting increased in parallel with ER membrane equivalents), whereas only background amounts of the protein cofractionated with mitochondria. By contrast, when both membranes are present, the preferred target for Cb5-D was clearly mitochondria because the majority of Cb5-D consistently fractionated with this organelle in a manner that paralleled pOCTgPA. Only when the relative amounts of ER membranes were increased to 12 or 24 equivalents was there a notable increase in the proportion of Cb5-D protein that cofractionated with ER membranes. Thus, Cb5-D targeting is highly specific for mitochondria.

The C Termini of Cb5 Proteins Contain Targeting Information That Is Both Necessary and Sufficient for Localization to Either ER or Mitochondria

To characterize the specific targeting information required for high fidelity sorting of Cb5 proteins to either the ER or mitochondria in plant cells, we conducted a series of targeting experiments using modified versions of myc-tagged Cb5-A and Cb5-D (Figures 4A and 4B). Removal of C-terminal sequences, including the TMD and tail regions from either Cb5-A or Cb5-D, resulted in mislocalization of both truncated proteins (Cb5-AΔ28 and Cb5-DΔ21) to the cytosol in BY-2 cells. Swapping the C termini of Cb5-A and Cb5-D, however, resulted in targeting of the hybrid proteins (Cb5-A/D and Cb5-D/A) to the mitochondria or ER, respectively. Similarly, the C termini of Cb5-A and Cb5-D directed GFP to either ER (GFP-Cb5-A) or mitochondria (GFP-Cb5-D). Expression of GFP-Cb5-A in BY-2 cells resulted in dramatic changes in ER morphology, as evidenced by numerous circular structures that were distributed uniformly throughout the cell (e.g., compare the calreticulin staining in Cb5-D/A and GFP-Cb5-A–transformed cells). These types of circular ER structures were observed also in cells expressing certain mutant versions of Cb5-A (e.g., Cb5-AΔtail and Cb5-A/D tail; discussed below) and are reminiscent of the concentric membrane whorls observed in yeast and mammalian cells (over)expressing other Cb5 and GFP fusion membrane proteins (Vergeres et al., 1993; Pedrazzini et al., 2001; Snapp et al., 2003). Although we did not investigate the mechanisms responsible for the formation of these ER whorl-like structures in BY-2 cells, they are most likely attributable to the oligomerization of cytosolic-facing portions of the expressed

Figure 3. (continued).

(C) Targeting of various Cb5 isoforms and pOCTgPA to microsomes and mitochondria in the same reaction. Translation reactions containing Cb5-A, Cb5-D, and pOCTgPA were added to mitochondrial import reactions containing mitochondria (50 μg of total protein) and either 0, 2, 4, 8, 12, or 24 equivalents of ER microsomes (Eq. ER). Mitochondria (M) and ER (E) were then separated by differential centrifugation, and the proteins in each pellet fraction were analyzed by SDS-PAGE/autoradiography.

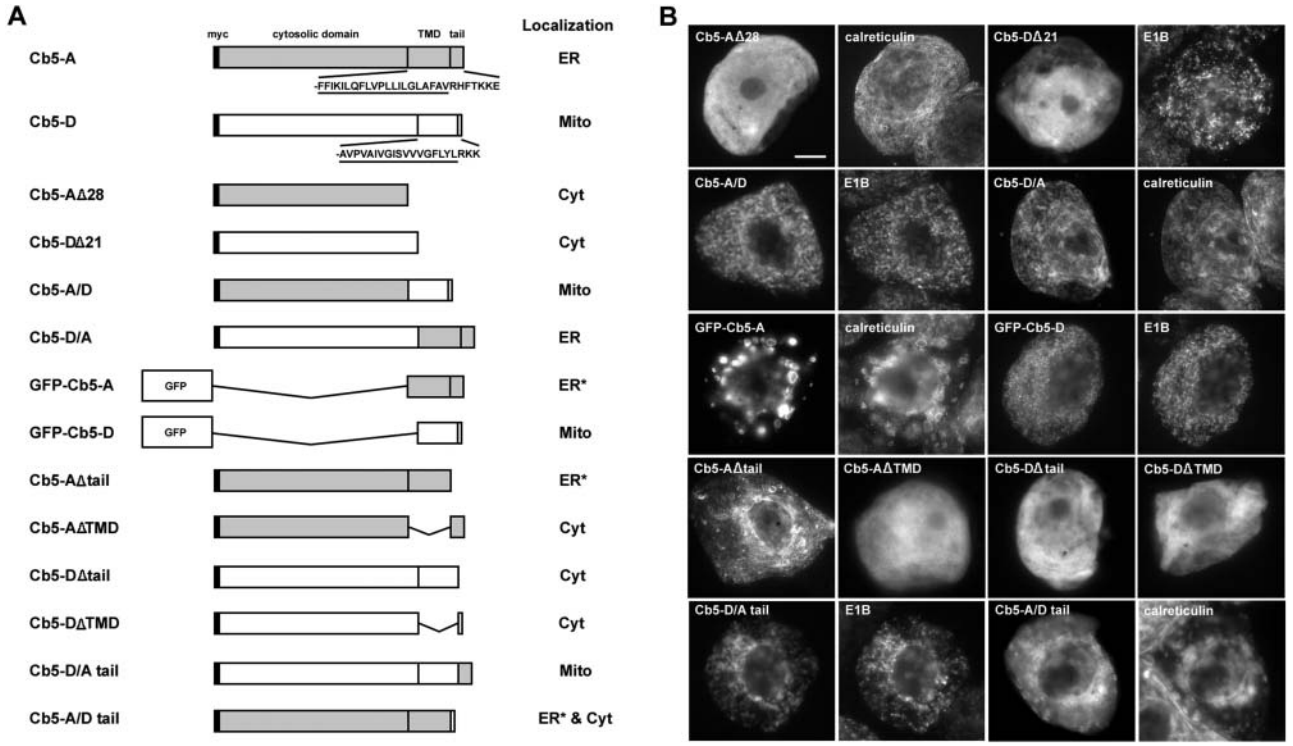

Figure 4. C-Terminal Targeting Signals in Cb5-A and Cb5-D.

(A) Schematic representations of wild-type and C-terminal mutant versions of Cb5-A and Cb5-D and their corresponding intracellular localization in transformed BY-2 cells as either ER, ER whorls (ER*), mitochondria (Mito), and/or cytosol (Cyt). Black boxes, N-terminal myc-epitope tag; gray boxes, Cb5-A sequences; open boxes, Cb5-D. Amino acid residues corresponding to the Cb5-A and Cb5-D C-terminal TMDs (underlined) and tail regions are also shown.

(B) Representative micrographs showing fluorescence patterns of various constructs illustrated in **(A)**. Each panel is labeled at the top left with either the name of the transiently expressed Cb5 or GFP-Cb5 construct or the name of the endogenous organelle marker protein (i.e., ER calreticulin or mitochondrial E1β) (co)immunostained in certain transformed cells. Bar = 10 μm.

membrane proteins, a process referred to as membrane zippering (Gong et al., 1996; Mullen et al., 2001; Lisenbee et al., 2003).

Because the data above indicated that the C-terminal sequences of Cb5-A and -D were both necessary and sufficient for localization of proteins to either the ER or mitochondria, we examined next the targeting function of the respective TMD and tail regions. Whereas Cb5-A lacking the tail (Cb5-AΔtail) remained localized to the ER (including ER whorls), Cb5-A without the TMD (Cb5-AΔTMD) was entirely mislocalized to the cytosol. On the other hand, both the TMD and tail sequences of Cb5-D were necessary for mitochondrial targeting, as evidenced by the mislocalization of Cb5-DΔtail and Cb5D-ΔTMD to the cytosol. Substitution of the Cb5-D tail with the Cb5-A tail (Cb5-D/A tail) had no obvious effect on mitochondrial localization, suggesting that the tail sequence of Cb5-A is compatible with mitochondrial targeting in the context of the Cb5-D TMD. The converse mutant Cb5-A/D tail, however, was localized to ER (including ER whorls) and cytosol, indicating that Cb5-D tail contained information that diminished, but did not abolish, ER sorting mediated by the Cb5-A TMD (cf. the localization of Cb5-A/Dtail and Cb5-AΔtail). In summary, these results demonstrate that targeting of Cb5 proteins to the ER requires sorting information present primarily in the TMD sequence, whereas localization of Cb5 to the mitochondria requires sorting determinants present in both the TMD and tail sequences.

Comparative Analysis of C-Terminal Sequences of Various Plant Cb5 Proteins

To determine whether the C-terminal TMDs and tails of ER and mitochondrial Cb5 isoforms contained distinctive features that might serve as organelle-specific targeting signals, we compared the C-terminal sequences of several known or putative ER and mitochondrial isoforms of plant Cb5s (i.e., proteins that were most similar with either the ER isoforms Cb5-A, -B, or -C or the mitochondrial isoform Cb5-D) (refer to phylogenetic tree shown in Figure 1B). As illustrated in Figure 5A, the most obvious difference between these two groups of proteins is that the lengths of the predicted TMD and tail sequences of the ER isoforms are consistently longer (21 and 7 to 9 amino acids, respectively) than the corresponding regions of the mitochondrial isoforms (18 and 3 amino acids, respectively). Despite these differences in length, the TMDs of ER and mitochondrial Cb5s share similar levels of overall hydrophobicity (data shown only for Cb5-A and Cb5-D;

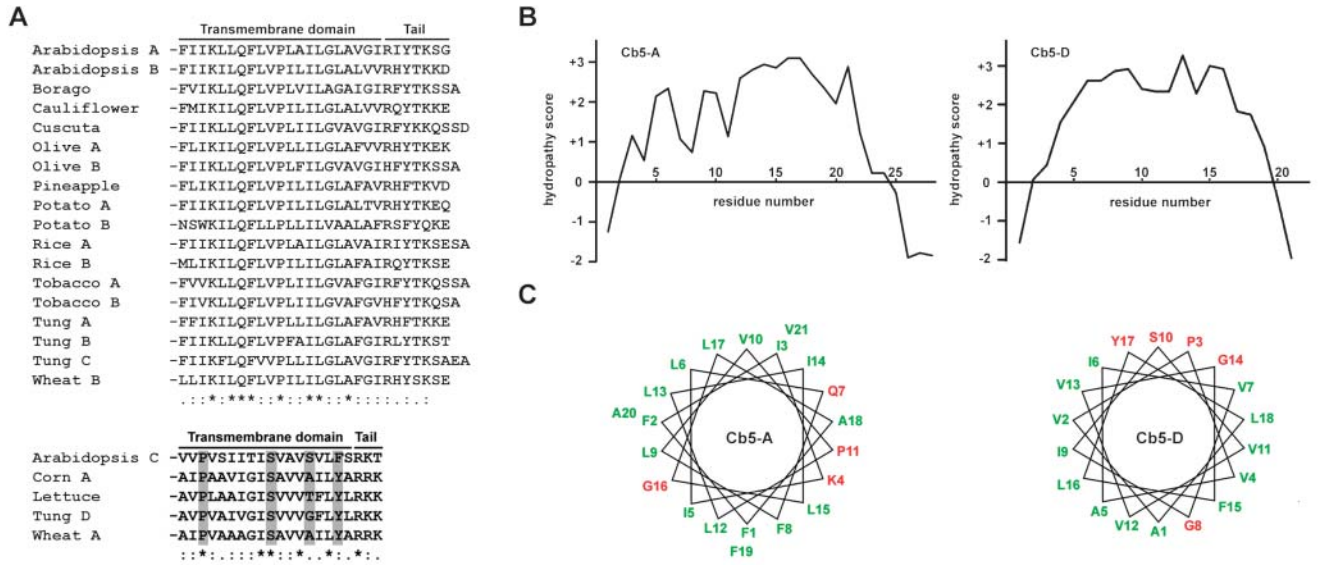

Figure 5. Comparisons of the C Termini of ER and Mitochondrial Isoforms of Cb5.

(A) Deduced amino acid sequence alignment of various known and putative ER (top group) and mitochondrial (bottom group) isoforms of plant Cb5. Predicted C-terminal TMDs and tail regions are indicated with lines above each group of proteins. Identical residues in each group are marked by asterisks, highly similar residues are indicated with colons, and similar residues are indicated by dots. Residues that are predicted to form a moderately hydrophilic face along the length of the TMD of all mitochondrial Cb5 isoforms are shaded (refer also to Figure 5C). Sequences were aligned using the ClustalW algorithm, and TMDs were identified using TMHMM (version 2.0).

(B) Hydropathy profiles for the C termini of Cb5-A and Cb5-D. The relative hydropathy score (according to the Kyte-Doolittle algorithm [Kyte and Doolittle, 1982]; hydrophobic >0 and hydrophilic <0) is plotted against the amino acid residues of the C-terminal segment of Cb5-A or Cb5-D. Hydropathy analysis was performed using the ProtParam program with a window of five amino acids to scan through the C-terminal sequence.

(C) α-Helical wheel projections of Cb5-A and Cb5-D TMD sequences. Hydrophobic residues in the TMD are green, and hydrophilic residues are red. Numbers next to each residue correspond to their position beginning at the N-terminal end of the TMD for Cb5-A (1 to 21 residues) or Cb5-D (1 to 18 residues).

Figure 5B). The TMDs of mitochondrial Cb5s, however, appear to be enriched in branched β-carbon–containing amino acids (i.e., Val and Ile), particularly toward the middle of the TMD sequence (Figure 5A). Neither group of proteins possesses TMDs exhibiting clear amphipathic characteristics. However, we identified a moderately hydrophilic face along the length of the TMD of mitochondrial Cb5 isoforms (data shown only for Cb5-A and Cb5-D, amino acids in red; Figure 5C). In addition to differences in length, the tail sequences of the two groups of Cb5 proteins show striking differences in the conservation of charged amino acids (Figure 5A). Each mitochondrial isoform contains a three–amino-acid-long tail sequence with at least two contiguous positively charged residues immediately adjacent to the TMD. By contrast, each ER isoform contains a tail sequence beginning with one or two positively charged amino acids followed by a hydrophilic sequence of varying length, composition, and net charge.

A Contiguous Dibasic Motif in the Tail of Mitochondrial Cb5 Proteins Is Essential for Targeting

Tung Cb5-D is the first mitochondrial-specific Cb5 isoform identified in plants; therefore, identification of the sequences required for mitochondrial targeting is of particular interest. We initially characterized the targeting information in the tail region of Cb5-D by analyzing a variety of mutations aimed at determining the optimal length, charge density, and location of the tail sequence relative to the TMD (Figures 6A and 6B). Successive deletions of amino acid residues from the C terminus of Cb5-D demonstrated that removal of either one (Cb5-D-RK) or two (Cb5-D-R) residues disrupted mitochondrial targeting and resulted in the mutant proteins being mislocalized to the cytosol, although in some cells a small proportion of Cb5-D-RK was observed to be targeted to both mitochondria and the cytosol (data not shown). Replacement of the tung Cb5-D tail sequence (-RKK) with the tail sequence of the Arabidopsis Cb5 isoform C (-RKT; refer to Figure 5A) or a modified version thereof (-TRK) resulted in mitochondrial localization, whereas the mutant Cb5-D-RTK mislocalized to the cytosol. Collectively, these results indicate that the tail sequence of a mitochondrial Cb5 protein must be at least three amino acids in length and that the sequence must contain a contiguous dibasic motif.

Acceptable degeneracy in the mitochondrial targeting signal of the Cb5-D tail was further investigated by substituting amino acids at each position with a variety of other conservative or nonconservative residues (Figure 6). Replacement of the Cb5-D C-terminal Lys with either Ala (Cb5-D-RKA) or Tyr (Cb5D-RKY) had no obvious negative effects on mitochondrial targeting, but substitution with Glu (Cb5-D-RKE) abolished mitochondrial targeting. The Lys at the −2 position could be functionally replaced by a positively charged His residue (Cb5-D-RHY), but

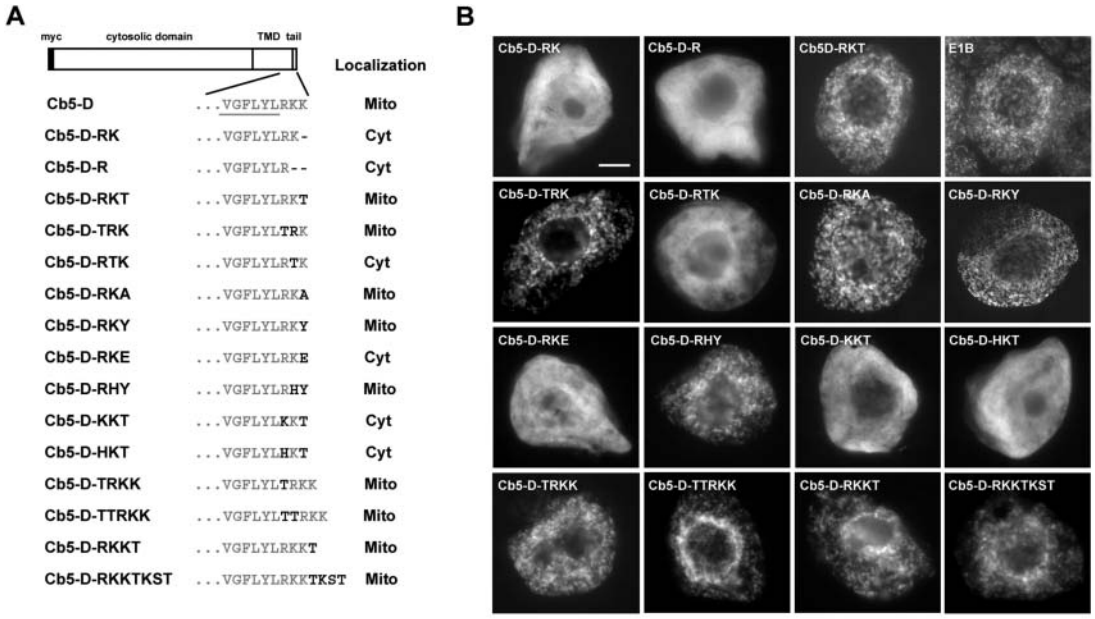

Figure 6. Characterization of the Targeting Information in the Tail Region of Mitochondrial-Localized Cb5 Proteins.

(A) Schematic representation of myc-tagged Cb5-D and the C-terminal sequences of either wild-type or mutant versions of myc-Cb5-D and their corresponding intracellular localization in transformed BY-2 cells as either mitochondria (Mito) or cytosol (Cyt). Wild-type Cb5-D C-terminal amino acid residues, including those in the TMD (underlined) and tail region, are shown in gray, and modified amino acid residues in the tail are shown in black and are bold.

(B) Representative fluorescence patterns attributable to various constructs illustrated in **(A)**. Each micrograph is labeled at the top left with either the name of the transiently expressed Cb5-D mutant construct or E1β, the endogenous mitochondrial marker protein (co)immunostained in the Cb5-D-RKT transformed cell. All staining patterns of expressed proteins were compared with the pattern of endogenous ER or mitochondrial marker proteins for determination of subcellular localization (data shown only for selected constructs). Bar = 10 μm.

replacement of the Arg residue at the −3 position with either Lys (Cb5-D-KKT) or His (Cb5-D-HKT) disrupted mitochondrial targeting, indicating that the Arg residue was essential for mitochondrial sorting of Cb5.

To determine if the positioning of the dibasic motif relative to the TMD was essential for efficient mitochondrial targeting, either one or two Thr residues were inserted into the Cb5-D sequence between the Leu at the C-terminal end of the TMD and the Lys at the −3 position of the tail (Figure 6A). Both Cb5-D-TRKK and Cb5-D-TTRKK localized to mitochondria in a manner similar to that of native Cb5-D. The mitochondrial localization of Cb5-D was preserved also when either a single Thr residue (Cb5-D-RKKT) or a short stretch of amino acids that were derived from the C-terminal end of Cb5-B (underlined, -RKKTKST) were appended to its C terminus, suggesting that the dibasic motif can function in targeting when positioned at least four amino acids upstream from the C terminus.

The TMD of Mitochondrial Cb5-D Contains Both Sequence-Specific and Physicochemical Targeting Information

The length of the Cb5-D TMD is three residues shorter than the TMDs of ER-localized isoforms of Cb5 (refer to Figure 5A). Increasing the length of the Cb5-D TMD from 18 to 21 amino acids by addition of three hydrophobic residues (-LIL-) resulted in targeting of the modified protein (Cb5-D-LIL^{21}) to the ER (Figure 7), demonstrating that a longer TMD sequence was indeed important for discriminating between the ER and mitochondrial targeting pathways. Replacement of the 18–amino acid mitochondrial TMD with 18 Leu residues (Cb5-D-polyL^{18}) or Ala, Leu, and Val repeats (Cb-5D-polyALV^{18}), however, also resulted in targeting of the modified proteins to the ER, indicating that length alone was not the sole discriminating factor for mitochondrial targeting. Interestingly, reversing the primary amino acid sequence of the Cb5-D TMD resulted in mislocalization of the mutant protein (Cb5-D-TMD^{Rev}) to the cytosol, indicating that mitochondrial targeting requires both a shorter TMD and specific amino acid sequences.

The minimal sequence information in the TMD of Cb5-D sufficient for mitochondrial targeting was investigated by restoring various wild-type Cb5-D residues in the context of Cb5-D-polyL^{18}, which localized to the ER (see above). Figure 7 shows that addition of the amino acid residues responsible for generating the moderate hydrophilic face on the Cb5-D TMD (i.e., the Pro, Ser, Gly, and Tyr residues at the 3rd, 10th, 14th, and 17th positions, respectively, of the 18–amino-acid-long TMD of Cb5-D; refer to Figures 5A and 5C) did not restore mitochondrial targeting (Cb5-D-PSGY). Mitochondrial targeting was not restored also when amino acids from the latter third of the Cb5-D TMD sequence were included in the context of Cb5-D-PSGY (Cb5-D-PSGY scan A). Only when wild-type amino acid sequences from either the middle

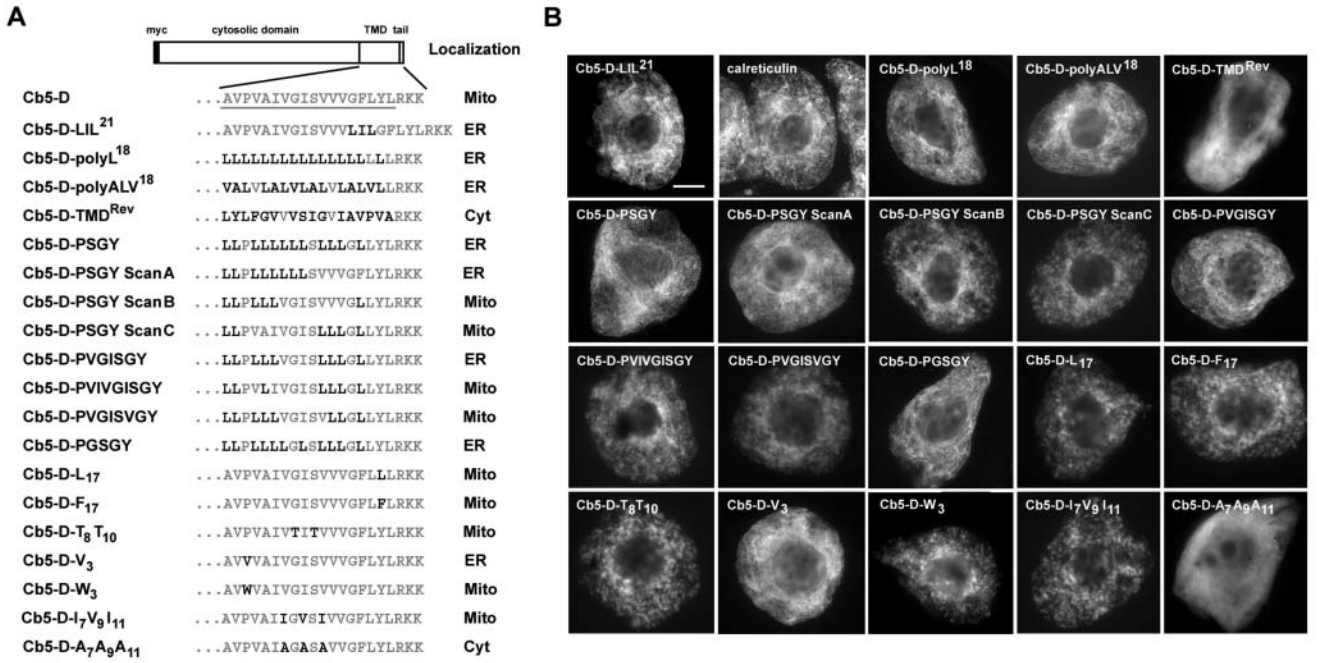

Figure 7. Characterization of the Targeting Information in the TMD of Mitochondrial-Localized Cb5 Proteins.

(A) Schematic representation of myc-tagged Cb5-D and the C-terminal sequences of either wild-type or mutant versions of myc-Cb5-D and their corresponding intracellular localization in transformed BY-2 cells as either ER, mitochondria (Mito), or cytosol (Cyt). Wild-type Cb5-D C-terminal amino acid residues, including those in the TMD (underlined) and tail region, are shown in gray, and modified amino acid residues in the TMD are shown in black and are bold.

(B) Representative fluorescence patterns attributable to various constructs illustrated in **(A)**. Each micrograph is labeled at the top left with either the name of the transiently expressed Cb5-D mutant construct or the name of the endogenous organelle marker protein (i.e., ER calreticulin or mitochondrial E1β) (co)immunostained in transformed cells. Bar = 10 μm.

or beginning of the Cb5-D TMD were added back to the Cb5-D-PSGY mutant was targeting to mitochondria observed (Cb5-D-PSGY scan B and Cb5-D-PSGY scan C). Reconstitution of the overlapping medial region shared by the Cb5-D-PSGY scan B and scan C mutants did not result in targeting to mitochondria (Cb5-D-PVGISGY), but additions of branched β-carbon–containing amino acids from Cb5-D either before (Cb5-D-PVIVGISGY) or after (Cb5-D-PVGISVGY) this shared medial region did restore mitochondrial targeting. Notably, Leu residues were not able to functionally replace the branched β-carbon–containing Ile and Val residues in the TMDs of the latter two minimal constructs (Cb5-D-PGSGY).

The contribution of individual amino acids and/or physicochemical properties to the mitochondrial targeting signal in the Cb5-D TMD sequence was evaluated further by mutating specific residues in the context of native Cb5-D. As shown in Figure 7, replacement of the Tyr residue located toward the C-terminal end of the hydrophilic face of the TMD (position 17) with either a hydrophobic Leu (Cb5-D-L_{17}) or hydrophobic, large/aromatic Phe (Cb5-D-F_{17}) had no effect on mitochondrial localization. Similarly, mitochondrial targeting of Cb5-D was not disrupted when two small/polar Thr residues were substituted for the hydrophilic Gly and Ser residues at positions 8 and 10, respectively (Cb5-D-T_8T_{10}). These latter data are significant because the Ser residue is predicted to be part of the hydrophilic face of the Cb5-D TMD (Figure 5C) and is conserved in the TMDs of all other mitochondrial Cb5 isoforms (Figure 5A). Targeting to mitochondria was disrupted, however, when the conserved Pro residue located toward the beginning of the hydrophilic face of the TMD (at position 3; Figure 5A) was replaced with Val (i.e., Cb5-D-V_3 localized to the ER). Interestingly, substitution of Pro at position 3 with Trp did not affect mitochondrial targeting (Cb5-D-W_3), suggesting that an aromatic amino acid residue can be tolerated at this position in the TMD. Finally, substitutions of the branched β-carbon–containing amino acids near the middle of the TMD with other hydrophobic branched β-carbon–containing residues had no effect on mitochondrial localization (Cb5-D-$I_7V_9I_{11}$), whereas replacement of the same Val and Ile residues with Ala residues completely abolished mitochondrial targeting (Cb5-D-$A_7A_9A_{11}$).

In summary, the results presented in Figure 7 indicate that the critical targeting information in the 18–amino-acid-long TMD of Cb5D includes a short sequence of hydrophilic residues that exists along one face of the helix and an enrichment of branched β-carbon–containing amino acids toward the middle of the TMD.

Characterization of Targeting Signals in the TMD and Tail Regions of ER-Localized Cb5s

To determine if the C termini of ER-localized Cb5 proteins, like their mitochondrial counterparts, contained distinct sequences

involved in targeting, we tested a variety of mutations aimed at determining the importance of amino acid composition, length, and physicochemical properties of the TMDs and tails in these proteins. As shown in Figures 8A and 8C, neither reversal of the 21–amino acid sequence of the Cb5-A TMD (Cb5-A-TMD^{Rev}) or replacement of the residues within the Cb5-A TMD with Leu (Cb5-A-polyL^{21}) had an obvious negative effect on ER localization, suggesting that specific amino acid sequences within the Cb5-A TMD are not essential for targeting. Removal of the tail sequence of Cb5-A-polyL^{21} (Cb5-A-polyL^{21}-Δtail) also had no effect on ER localization, which was consistent with previous observations for the ER localization of native Cb5-A lacking its tail sequence (Cb5-AΔtail, Figure 4). Truncation of the polyleucine TMD within the context of Cb5-A-polyLΔtail revealed that whereas a TMD of only 18 Leu residues remained sufficient for ER targeting (Cb5-A-polyL^{18}-Δtail), TMDs of either 14 or 10 Leu were not sufficient (Cb5-A-polyL^{14}-Δtail and Cb5-A-polyL^{10}-Δtail, respectively).

That the tail region of Cb5-A was neither necessary nor sufficient for ER targeting (Figure 4), but was capable of targeting a modified version of Cb5-D to mitochondria (Cb5-D/A tail; Figure 4), was somewhat surprising given the relative importance of this region in the sorting of mammalian Cb5 ER isoforms (Mitoma and Ito, 1992; Borgese et al., 2001). One possible explanation of these apparently contradictory data was that the dibasic sequence -RH- within the Cb5-A tail (underlined, -RHFTKKE)

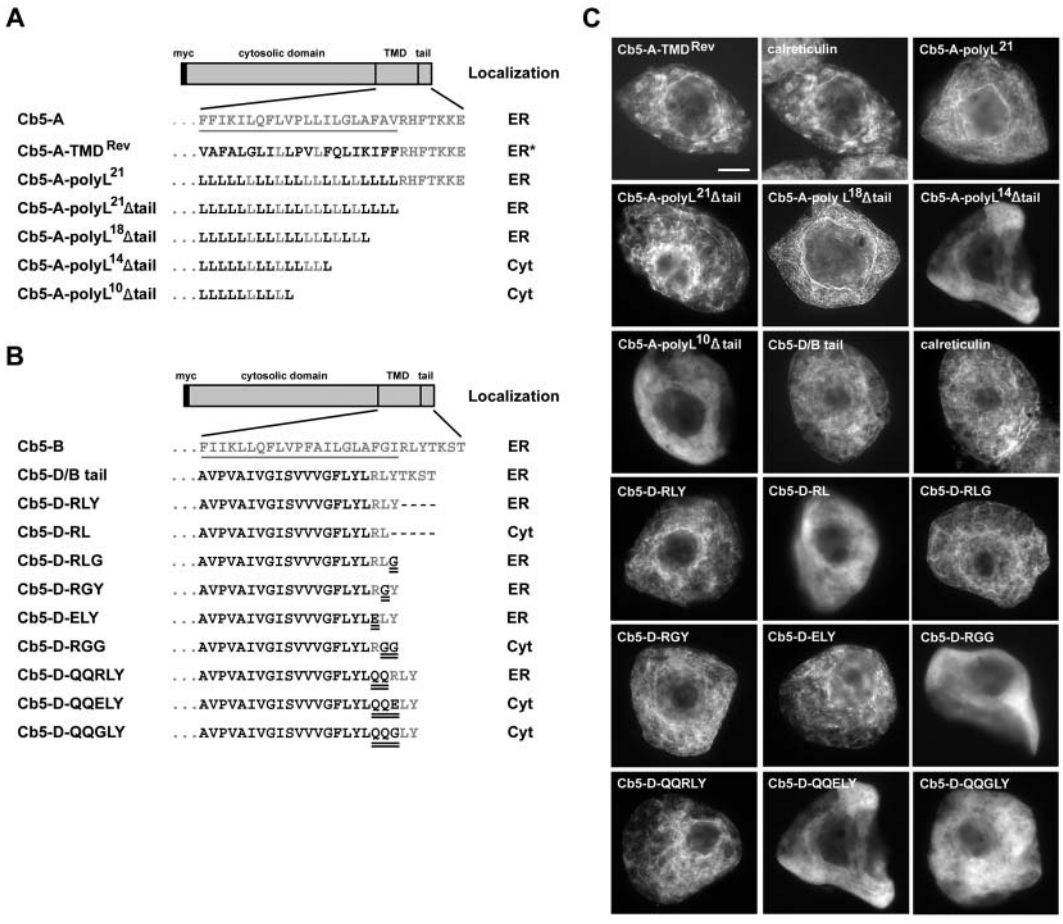

Figure 8. Characterization of the Targeting Information in the TMD and Tail Regions of ER-Localized Cb5 Proteins.

(A) Schematic representation of myc-tagged Cb5-A and the C-terminal sequences of either wild-type or mutant versions of myc-Cb5-A and their corresponding intracellular localization in transformed BY-2 cells as either ER, ER whorls (ER*), or cytosol (Cyt). Wild-type Cb5-A C-terminal amino acid residues, including those in the TMD (underlined) and tail region, are shown in gray, and modified amino acid residues in the TMD are shown in black and are bold.

(B) Schematic representation of myc-tagged Cb5-B and the C-terminal sequences of either wild-type myc-Cb5-B or mutant versions of myc-Cb5-D/B fusion proteins. Also shown is the intracellular localization of each construct in transformed BY-2 cells as either ER or cytosol. Wild-type Cb5-B and Cb5-D amino acid residues, including those in the TMD (underlined), are shown in gray and black, respectively, and modified Cb5-B amino acids in the tail region of Cb5-D/B mutant fusion proteins are in black and are double underlined.

(C) Representative fluorescence patterns attributable to various constructs illustrated in **(A)** and **(B)**. Each micrograph is labeled at the top left with either the name of the transiently expressed Cb5-A or Cb5-D mutant constructs or calreticulin, the endogenous ER marker protein (co)immunostained in certain transformed cells. Bar = 10 μm.

functioned, at least within the context of the Cb5-D TMD, as a cryptic mitochondrial targeting signal and that the targeting information in the Cb5-A tail was actually bifunctional depending upon its protein context. To test this hypothesis, we examined whether the tail sequence of another Cb5 ER isoform, specifically one that was lacking a putative cryptic dibasic mitochondrial targeting signal in its tail, was sufficient for sorting to the ER. As shown in Figures 8B and 8C, the tail sequence of tung Cb5-B, which lacks a contiguous dibasic motif (-RLYTKST), was indeed capable of redirecting the Cb5-DΔtail mutant (Cb5-D/B tail) from the cytosol to the ER. These data support the hypothesis that both the TMD and tail region of an ER-localized Cb5 can indeed function, at least when in the proper context, as separate ER targeting signals.

To determine the minimal length of the tail sequence required for ER targeting, progressive deletions were made to the tail of Cb5-B in the context of the Cb5-D/B tail mutant (Figures 8B and 8C). Whereas deletion of the C-terminal four residues from Cb5-D/B tail had no effect on ER targeting (Cb5-D-RLY), deletions of the C-terminal five residues abolished ER targeting (Cb5-D-RL), indicating that a minimum of three amino acids within the tail sequence were sufficient for targeting Cb5 to the ER. Notably, the Cb5-D-RLY tail sequence contained an -R/H-x-Y/F- motif present in the tails of all other ER-localized plant Cb5s (Figure 5A), suggesting that this motif represents a minimal sequence-specific ER targeting signal. Replacement of individual amino acid residues within the tail of Cb5-D-RLY with a variety of structurally diverse residues, however, did not abolish ER localization. That is, substitution of either Tyr at the −1 position or Leu at the −2 position with Gly (Cb5-D-RLG or Cb5-D-RGY, respectively), or substitution of Arg at the −3 position with Glu (Cb5-D-ELY), all resulted in localization of the mutant proteins in ER. Only when both residues at the −1 and −2 positions were replaced with Gly was the resulting mutant protein (Cb5-D-RGG) mislocalized to the cytosol, suggesting that the C-terminal residues in the -RLY sequence of the Cb5-B tail function in a cooperative manner as an ER targeting signal. Insertion of a -QQ- linker sequence between the Cb5-D TMD and the -RLY sequence had no obvious effects on ER localization (Figure 8), but replacement of the Arg residue at the −3 position with either a Glu (Cb5-D-QQELY) or Gly (Cb5-D-QQGLY) resulted in mislocalization to the cytosol (Figure 8), indicating that the highly conserved Arg residue in the Cb5-B tail was indeed important for ER localization.

In summary, the data presented in Figure 8 demonstrate that the targeting signals responsible for the localization of a Cb5 protein to the ER include a TMD sequence of sufficient length and overall hydrophobicity and a tail sequence that includes a conserved -R/H-x-Y/F- motif.

DISCUSSION

Comparisons of Cb5 Targeting among Evolutionarily Diverse Organisms

In this study, four different isoforms of tung Cb5 were identified, and examinations of their subcellular localization in BY-2 cells and assembly into isolated membrane/organelle fractions in vitro revealed they were targeted specifically to either the ER or mitochondria. These data are novel, especially for Cb5-D, because no other plant Cb5s identified to date have been experimentally demonstrated, nor proposed, to be targeted exclusively to mitochondria. Instead, other Cb5s from plants have been reported to be localized either to the ER alone (Smith et al., 1994) or to the ER as well as to mitochondria as a result of the dual distribution of a single gene product (Zhao et al., 2003). The characterization of mitochondrial and ER tung Cb5 isoforms, plus the identification of other putative mitochondrial and ER Cb5 proteins in different plant species, including tobacco (*Nicotiana tabacum*), wheat (*Triticum aestivum*), and Arabidopsis (Figure 5A), suggests that the differential localization of Cb5s is a well-conserved feature among plants.

The existence of multiple Cb5 isoforms also appears to be a recent evolutionary trend because mammals, like plants, have at least two differential localized forms of the enzyme, whereas in yeast and other lower eukaryotes, only ER-localized Cb5s have been identified (Schenkman and Jansson, 2003). It appears that mitochondrial Cb5s arose in higher eukaryotes from their ER-localized counterparts, and in lower eukaryotes other proteins can serve as functional equivalents of mitochondrial Cb5 (e.g., flavocytochrome b_2 in yeast mitochondria) (Mathews, 1985).

Results from our in vitro experiments suggest also that the targeting factors responsible for the localization of Cb5 proteins, although not yet identified in any eukaryotic organism, are conserved between plants and mammals because tung Cb5 isoforms A and D targeted to mammalian ER and mitochondria, respectively (Figure 3). However, subtle differences in the in vitro targeting behavior of plant and mammalian Cb5s suggest that the *cis*-acting targeting signals for these proteins function in slightly different ways. For example, both ER and mitochondrial isoforms of mammalian Cb5 proteins are known to integrate in a promiscuous and spontaneous manner into membranes in vitro (Remacle, 1978; Enoch et al., 1979; Kim et al., 1997; Borgese et al., 2001), whereas plant Cb5 proteins retain their targeting fidelity in vitro (Figure 3). These data suggest that despite an overall similarity in the machinery responsible for Cb5 import in plants and mammals, the targeting signals of plant Cb5 proteins have acquired additional information that ensures high fidelity association with the correct organelle, while avoiding spurious interactions with other types of membranes. The plant Cb5 proteins, in combination with in vitro biochemical studies, should now facilitate a detailed analysis of the cytosolic factors, nucleotide and/or energy requirements, and membrane protein machinery required for selectivity in targeting and insertion of TA membrane proteins into either ER or mitochondrial outer membranes. These studies are currently underway in our laboratories.

The apparent need for a higher fidelity sorting mechanism for plant Cb5 proteins may be because of the presence of plastids in plant cells, which represent an additional potential recipient organelle for all newly synthesized, posttranslationally targeted proteins. Indeed, this form of refinement in the targeting pathways in plant cells because of the presence of plastids has been suggested also by Lithgow and coworkers (Macasev et al., 2000). These authors noted that the mitochondrial machinery required for matrix protein import was more diverged in plants in

comparison with mammals and yeast and that these differences in the plant import complex may provide for better discrimination between the presequences of mitochondrial- and plastid-targeted matrix proteins, which are structurally similar. Our data suggest that the targeting signals of plant TA proteins may have evolved in a similar fashion to provide better discrimination between the mitochondria, ER, and other organelles of the plant cell.

Our data indicate also that the targeting mechanisms responsible for the sorting of mitochondrial TA proteins in plants may have diverged compared with those in yeast. Evidence in support of this premise was provided by our assays of Cb5 function in *Saccharomyces cerevisiae*. Each of the tung Cb5 proteins complemented yeast Cb5 activity, as evidenced by restored FAD2 activity when coexpressed with tung FAD2 in a mutant Δ*CYB5* strain (Figure 1D). Although these functional complementation results for Cb5 isoforms A, B, and C were expected based upon their localization in the ER in plant cells (Figure 2), the complementation of FAD2 activity by the mitochondrial isoform Cb5-D was surprising. Plant FAD enzymes are localized exclusively in the ER in both plant and yeast cells (Dyer and Mullen, 2001; McCartney et al., 2004), and the ability of Cb5-D to stimulate FAD2 activity suggested that either a proportion of Cb5-D (mis)localized to the ER in yeast cells or that this isoform could donate electrons to ER-bound FADs in *trans* from the mitochondrial surface. Immunofluorescence microscopic analysis of yeast cells revealed, however, that all four tung myc-tagged Cb5 isoforms localized exclusively to the ER (our unpublished data), indicating that differences in either yeast mitochondrial TA import machinery and/or the *cis*-acting targeting signals of Cb5-D prevented its sorting to mitochondria. The future identification of the cellular machinery involved in mitochondrial TA protein targeting in yeast and plants and a comparative analysis of the mitochondrial targeting signals for yeast and plant TA proteins will undoubtedly provide a better understanding of the differences in the TA protein targeting pathways in these organisms.

Unique Aspects of Plant Cb5 Targeting Signals and Implications for the Biogenesis of TA Membrane Proteins in Plant Cells

In this study, a comprehensive mutagenic analysis of ER and mitochondrial-localized Cb5 proteins provided important insight to the precise nature of the targeting signals required for entry of TA proteins into either the ER or mitochondrial targeting pathways in plant cells. Overall, we showed that several features of the ER and mitochondrial targeting signals for tung Cb5 are unique when compared with the targeting signals reported previously for mammalian and yeast TA proteins. For example, there is general agreement that the targeting information of mammalian and yeast TA proteins is not contained in discrete signals but instead is the combination of TMD length and the degree of flanking positively charged residues (Wattenberg and Lithgow, 2001; Borgese et al., 2003). Specifically, those proteins with short TMDs (<20 residues) flanked by several basic residues are usually targeted to mitochondria, whereas proteins lacking this type of physicochemical information are targeted by default to the ER. Our data indicate that this general model does not adequately account for the targeting of plant Cb5s and that, instead, there exists discrete signals in these proteins that function in combination with physicochemical characteristics for their proper differential localization. For instance, although plant Cb5s either demonstrated or proposed to be localized to the mitochondria have shorter TMDs compared with their ER-localized counterparts (18 to 19 versus 21 residues; see Figure 5A), this conserved physicochemical feature did not ensure mitochondrial sorting; replacement of the Cb5-D TMD with other 18–amino-acid-long TMDs, including a reversed Cb5-D TMD sequence (Cb5-D-TMD^{Rev}) or an artificial TMD (i.e., Cb5-D-polyL^{18} and Cb5-D-polyALV^{18}), disrupted mitochondrial targeting even though the C-terminal tail remained intact (Figure 7). Instead, mitochondrial targeting of Cb5 required a TMD sequence composed of specific types of amino acids, including a conserved Pro residue, which was part of a short hydrophilic surface situated on the same face of the TMD, as well as an enrichment of branched β-carbon–containing amino acids toward the middle of the TMD. Mitochondrial targeting of Cb5 also required both sequence-specific and physicochemical characteristics within the tail region; the tail sequence must be at least three amino acids long and contain a contiguous dibasic motif in which one of the positively charged amino acids must be an Arg residue, and the third position cannot be occupied by a negatively charged residue (Figure 6). Although these different targeting elements in the TMD and tail of mitochondrial Cb5 operated in a cooperative manner, their precise functional and structural roles are difficult to predict without, for example, molecular dynamic simulations from the crystal structures of the wild-type and mutant proteins or their interactions with cognate receptors. Nonetheless, they do clearly illustrate that the targeting information in plant mitochondrial Cb5 is more complex than that previously reported for mammalian Cb5s or other TA proteins in general.

ER targeting signals of plant Cb5, although more broadly defined than the mitochondrial targeting signals, are also slightly different than their mammalian counterparts. For example, ER targeting in both plant and mammalian cells required a stretch of hydrophobic amino acids of sufficient length for targeting to the ER (Figure 8; Smith et al., 1994; Whitley et al., 1996), yet not all hydrophobic amino acid sequences were capable of inserting into ER membranes in plant cells. Specifically, removal of the tail sequence from mitochondrial Cb5-D (Cb5-DΔtail) left intact the 18–amino-acid-long TMD with an overall hydrophobicity that was comparable to that of its ER-localized Cb5 counterparts; therefore, the modified protein should have been localized to the ER. Instead, the protein remained in the cytosol (Figure 4), unless an ER Cb5 tail sequence was appended to the TMD (Figure 8B). Apparently, unique sequence and physicochemical features of the Cb5-D TMD not only act as positive signals that promote mitochondrial targeting, but serve also as negative signals that effectively prevent any so-called default targeting to the ER.

While the length and overall hydrophobicity of the TMD appear to be the most important determinants in ER targeting of Cb5s, the tail sequences of these proteins also appear to play a role in their proper localization. For instance, we showed that the tail sequences of plant Cb5 ER isoforms contain a targeting signal that is sufficient for sorting to the ER (i.e., addition of the Cb5-B

tail sequence to a Cb5-D mutant lacking its own tail region, and which is exclusively localized to the cytosol, resulted in the hybrid protein being targeted to ER) (Cb5-D/B tail, Figure 8B). Further mutagenic analysis of the Cb5-B tail region in the context of the Cb5-D TMD revealed that a conserved -R/H-x-Y/F- motif, found in all other plant ER Cb5 tail sequences, was the minimally sufficient sequence for ER targeting (Figure 8B). Interestingly, whereas nonconserved amino acid substitutions were tolerated within the -R/H-x-Y/F- motif, this was not likely because of functional degeneracy, but rather an extension of the shorter Cb5-D TMD by the appended -RLY motif and, thus, sorting of the mutant protein to the ER by the default pathway because of the presence of a longer TMD sequence. Evidence in support of this premise was obtained using a modified version of the Cb5-D-RLY mutant in which a -QQ- linker sequence was added between the TMD and -RLY tail sequence (Cb5-D-QQRLY; Figure 8B), which would serve to restrict the length of the hydrophobic membrane-spanning domain to 18 residues but preserve the α-helical nature at the C-terminal end of the protein (Deber and Li, 1995). Although Cb5-D-QQRLY was still efficiently targeted to the ER, replacement of the Arg at the -3 position with either a negatively charged Glu or a neutral Gly abolished ER targeting (Figure 8B). These and other results confirm the importance of the conserved residues in the -R/H-x-Y/F- motif and that this sequence is a basis for predicting the localization of Cb5 proteins to the ER in plant cells. Overall, the role of the tail sequences in ER Cb5s is likely related to increasing ER targeting efficiency or, as reported recently for the rat ER Cb5 isoform (Tanaka et al., 2003), facilitating membrane integration and assembly. It is also conceivable that the more complex targeting signals (i.e., distinct targeting elements in both the TMD and tail) of plant Cb5 proteins, as described above, have evolved to allow for better discrimination between ER, mitochondrial, and, unique to plant cells, plastid targeting pathways and that these signals provide higher fidelity/specificity with the receptor machinery of the various organelles that can acquire TA membrane proteins.

What now remains to be determined is whether the targeting signals characterized here for Cb5 form a consensus sequence for all plant mitochondrial and ER TA proteins, a task that will require the identification of other plant TA proteins and characterization of their targeting signals. These types of studies will clearly have an impact on our understanding of a multitude of cellular processes because a recent bioinformatics search of the Arabidopsis genome suggests that there are >300 TA proteins in the Arabidopsis proteome (P.K. Dhanoa and R.T. Mullen, unpublished data).

Implications of Cb5 Biogenesis for Storage Oil Biosynthesis and Other Cellular Processes

The biosynthesis of storage oils in developing seeds is a highly coordinated event that requires the involvement of proteins located in at least three different organelles, including plastids, the site of fatty acid biosynthesis, the ER, where most fatty acid modifications take place, and oil bodies, where fatty acid storage occurs (Ohlrogge and Browse, 1995). Approximately 50 years of intensive biochemical research has provided the details of the metabolic pathways in each of these compartments, and more recent efforts in gene cloning have yielded many of the enzymes involved in these processes. However, despite these advances, little is known about the targeting, assembly, and regulation of lipid biosynthetic enzymes. We identified and characterized four isoforms of tung Cb5, including three isoforms localized to ER and a fourth isoform localized to mitochondria. Although the exact function and tissue specificity of the mitochondrial-localized Cb5 isoform in plant cells is presently unclear, it is conceivable that it is involved in the reduction of ascorbate, similar to the role of the mammalian mitochondrial-localized Cb5 (Ito et al., 1981). Plant ER-localized Cb5s, on the other hand, are well known to provide electrons to a variety of ER-localized enzymes, including FAD and FAD-like enzymes (Figure 1D; Smith et al., 1990, 1992; Bafor et al., 1993; Napier et al., 2003). It is presently unclear, however, why tung and other plants should express multiple isoforms of Cb5 localized to the ER, especially because in mammalian or yeast cells there is only one ER-localized isoform. One hypothesis is that the various plant ER Cb5 isoforms have subtle structural differences that allow them to preferentially interact with other specific enzymes within the ER. Our functional complementation data in yeast cells suggest that this is not the case for FAD2 or FADX because these enzymes produced similar amounts of fatty acid products regardless of which Cb5 isoform was included in the assay (Figure 1D; data not shown). It is possible, however, that other FADs or ER-localized enzymes require a specific Cb5 isoform for their optimal enzyme activity. In support of this possibility, de Vetten et al. (1999) characterized a cytochrome P450 in petunia (*Petunia hybrida*) that requires a specific Cb5 isoform for production of pigments in flower tissues and showed that disruption of this Cb5 affected color formation but did not affect the activity of other P450 enzymes. We are currently exploring the physiological importance of the multiple tung Cb5 isoforms and the premise that their specific enzyme partners include members of the P450 protein family.

METHODS

Recombinant DNA Procedures and Reagents

Standard recombinant DNA procedures were performed as described by Sambrook et al. (1989). Molecular biology reagents were purchased either from New England Biolabs (Beverly, MA), Promega (Madison, WI), or Perkin-Elmer Biosystems (Mississauga, Canada). Synthetic oligonucleotides were synthesized by either Invitrogen (Frederick, MD) or the University of Guelph Laboratory Services (Guelph, Canada), DNA was isolated using Qiagen reagents (Mississauga, Canada), and dye terminated cycle sequencing was used with an Applied Biosystems Model 377 automated sequencer (Perkin-Elmer Biosystems) to verify all DNA constructs. Mutagenesis was performed using appropriate complementary forward and reverse mutagenic primers and the QuikChange site-directed mutagenesis kit according to the manufacturer's instructions (Stratagene, La Jolla, CA). PCR and rapid amplification of cDNA ends were performed with either a Hybaid PCR Express thermal cycler (Continental Lab Products, San Diego, CA) or a GeneAMP PCR System 2400 (Perkin-Elmer Biosystems). All of the modified versions of tung Cb5 proteins described in this article were generated using either site-directed mutagenesis or synthetic double-stranded (complementary) oligonucleotides based on sequences provided in GenBank. A complete description

of the construction of these plasmids and other plasmids described below, along with the sequences of all oligonucleotide primers, are available upon request.

Cb5 Cloning and Plasmid Constructions

A tung (*Aleurites fordii* Hemsl.) seed cDNA library was screened using PCR with a degenerate 3′ primer (5′-TCYTCRAARTCRTTIGTNGCRTCYTT-3′) that corresponded to a conserved region of the Cb5 protein family and a 5′ primer that bound to adjacent phagemid DNA. Full-length cDNAs encoding Cb5-A, -B, -C, and -D were then obtained by rapid amplification of cDNA ends using PCR and internal primers specific to each cDNA.

The construction of yeast expression plasmids containing the tung Cb5 open reading frames (ORFs) was performed as follows. First, each Cb5 ORF was amplified using PCR with appropriate forward and reverse primers that introduced an in-frame *Nhe*I and *Xba*I site 5′ and 3′ of the start and stop codons, respectively. Next, PCR products were gel purified and subcloned into the galactose-inducible yeast expression vector pYES2.1 (2 μm, *URA*) (Invitrogen). These plasmids were then digested each with *Nhe*I and *Xba*I, and the resulting DNA fragments were gel purified and ligated into *Xba*I-digested pRTL2-mycX. The pRTL2-mycX plasmid is a modified version of the plant expression vector pRTL2ΔN/S (Lee et al., 1997) that includes sequences encoding an initiator Met, Gly linkers, and the myc-epitope tag (underlined, MGEQKLISEEDLG-; Fritze and Anderson, 2000) followed by an in-frame *Xba*I site that allows for the convenient ligation of passenger coding sequences. The construction of other yeast expression vectors (pYES2.1) containing myc-tagged versions of the four tung Cb5 ORFs was performed using PCR with the appropriate forward and reverse primers and the pRTL2-myc-Cb5 plasmids as template DNA. Plasmids containing either a GFP-Cb5-A or GFP-Cb5-D fusion protein were generated by ligating the *Nhe*I-*Xba*I fragments from modified versions of pRTL2/myc-Cb5A and pRTL2/myc-Cb5D (both containing a unique *Nhe*I site immediately 5′ of the sequences coding for the TMD) and encoding the C-terminal 28 and 21 amino acids (TMD and tail) of either Cb5-A and Cb5-D, respectively, into *Xba*I-digested pRTL2/GFP-*Xba*I. The plasmid pRTL2/GFP-*Xba*I is a general purpose GFP fusion cassette vector whereby an in-frame *Xba*I site was substituted for sequences encoding the GFP stop codon (Lisenbee et al., 2003). Plasmid pRTL2/GFP-Tom22, containing the Tom22 ORF encoded on chromosome 5 (Tom22 V; Macasev et al., 2000) appended to the C terminus of the GFP ORF, was constructed as follows. First, the Tom22 ORF was amplified from pZL1/AtTOM22-V (obtained from the ABRC) using PCR with appropriate forward and reverse primers that introduced an in-frame *Xba*I at the Tom22 start codon. Next, the PCR products were subcloned into pCR2.1 (Invitrogen), and the resulting plasmid, pCR2.1/Tom22, was digested with *Xba*I. The *Xba*I DNA fragments were ligated into *Xba*I-digested pRTL2/GFP-*Xba*I to yield pRTL2/GFP-Tom22. The construction of yeast expression plasmids containing ER-localized tung FAD2 has been described previously (Dyer et al., 2002).

The vectors pSPUTK (Falcone and Andrews, 1991) and pSPUTK-*Bgl*II (McCartney et al., 2004) containing the SP6 promoter were used for in vitro membrane insertion experiments. Plasmid pSPUTK/myc-Cb5-A was generated by ligating the *Nco*I-*Xba*I fragment from pRTL2/myc-Cb5-A into *Nco*I-*Xba*I–digested pSPUTK. To construct pSPUTK/Cb5-A, DNA sequences encoding the Cb5-A myc-epitope tag in pSPUTK/myc-Cb5-A were deleted using site-directed mutagenesis. Plasmid pSPUTK-*Bgl*II/Cb5-D was constructed in two steps. First, DNA sequences encoding the Cb5-D ORF were amplified from pRTL2/myc-Cb5-D using PCR along with a mutagenic forward primer that introduced a *Bgl*II site immediately 3′ of the myc-epitope coding sequence and 5′ of the Cb5-D initiation Met, and a reverse primer that was complementary to sequences 3′ of the Cb5-D stop codon and a unique *Xba*I site. The resulting PCR products were gel purified and subcloned into pSPUTK-*Bgl*II. Next, a Kozak's initiation site (-CCATGG-; Kozak, 1999) was introduced into the Cb5-D ORF using site-directed mutagenesis and appropriate forward and reverse complementary primers. The construction of pSP/CytoB5 (Janiak et al., 1994a) containing the rat liver Cb5 ORF, pSPUTK/Vamp2 (Kim et al., 1999) encoding rat Vamp2, and pSP/pOCTgPA (Janiak et al., 1994a) encoding the 32 amino acids of the pOCT mitochondrial presequence and 29 amino acids of the mature protein followed by the IgG binding domain (amino acids 23 to 271) of protein A (gPA) from *Staphlococcus aureus* have been described elsewhere.

Targeting to Membranes in Vitro

Salt-extracted pig pancreatic ER membranes (microsomes) and rat liver mitochondria were prepared as previously described (Walter and Blobel, 1983; Janiak et al., 1994b). Plasmids were transcribed in vitro using SP6 polymerase (MBI Fermentas, Burlington, Canada), and RNAs were translated using rabbit reticulocyte lysate in the presence of ^{35}S-Met (Perkin-Elmer Biosystems-NEN) (Perara and Lingappa, 1985). To ensure that only posttranslational targeting occurred, ribosomes were removed from translation reactions before the addition of microsomes or mitochondria by centrifugation at 200,000*g* for 10 min. In addition, for the translation reactions yielding Cb5-D, the globin from the reticulocyte lysate was removed by diethylaminoethyl Sepharose chromatography because it migrates close to the same position as Cb5-D on SDS-PAGE and distorts the lane because of its high concentration (~10 mg mL^{-1}). Removing the globin from these reactions therefore improved quantification of the Cb5-D protein band but reduced the synthetic capacity of the lysate significantly. One equivalent of microsomes (defined as 100 fmol of SRP receptor α-subunit; Andrews et al., 1989) or one equivalent of mitochondria (defined as 50 μg of total mitochondrial protein) were then added to translation reactions and incubated for 1 h at 24°C. Import reactions with microsomes were layered onto a 0.5 M sucrose cushion, and membranes were pelleted by centrifugation at 100,000*g* for 10 min (McCartney et al., 2004). Gradients were fractionated into top and middle fractions (representing soluble proteins), and a bottom fraction was obtained by solubilizing pelleted material (including microsomes and microsomal-associated proteins) in SDS loading buffer. Import reactions with mitochondria were layered onto a 0.5 M sucrose cushion and centrifuged at 16,000*g* for 10 min. Top and middle fractions were collected, and the mitochondrial pellet was washed twice in 0.5 M potassium acetate, centrifuged, and resuspended in loading buffer. Integration of proteins into microsomal or mitochondrial membranes was determined by washing pelleted materials in a bottom fraction with either alkaline sodium carbonate, sodium thiocyanate, or sodium chloride as previously described (Andrews et al., 1992). All centrifugation steps with microsomes and mitochondria were performed using a TL100 ultracentrifuge (Beckman, Mississauga, Canada) and a tabletop microfuge (Eppendorf, Hamburg, Germany), respectively. Equivalent amounts of each fraction corresponding to original translation reactions were analyzed by SDS-PAGE using a Tris-Tricine buffer system (Schägger and von Jagow, 1987). Labeled proteins were visualized and quantified using a Molecular Dynamics Storm PhosphorImager with allied software (version 5.0) (Amersham Biosciences, Baie d'Urfé, Canada).

For competition experiments, either mitochondria alone (50 μg) or mitochondria (50 μg) plus increasing (2, 4, 8, 12, or 24) equivalents of microsomes were added to mixed translation reactions and incubated for 1 h at 24°C as described previously (Janiak et al., 1994b). Microsomes were then separated from mitochondria in import reactions by the addition of EDTA to 50 mM and potassium acetate, pH 7.5, to 0.5 M, followed by centrifugation (12,000*g* for 5 min) over a 0.5 M sucrose cushion. The resulting pellet containing mitochondria and mitochondrial-bound proteins was washed with import buffer plus EDTA and potassium acetate, centrifuged as above and resuspended in SDS loading bufffer. Microsomes and microsomal-bound proteins in the supernatant were

collected by centrifugation (100,000*g* for 15 min) through a sucrose cushion. Labeled proteins from both mitochondrial and ER pellet fractions were analyzed by SDS-PAGE/autoradiography. The data shown for all in vitro membrane insertion reactions are representative of three independent experiments.

Plant Material, RNA Extractions, and RNA Gel Blotting

Tung leaves and seeds were harvested from the orchards of American Tung Oil (Lumberton, MS). All samples were immediately frozen in liquid N_2 and stored at −80°C until used. Total RNA was extracted using the method of Bugos et al. (1995), then 10 μg of leaf or seed RNA was separated by agarose gel electrophoresis, transferred to Nytran positively charged membrane (Schleicher and Schuell, Keene, NH), and blotted with full-length digitonin-labeled riboprobes derived from each Cb5 ORF (Roche, Indianapolis, IN) under high stringency conditions (Ambion Northern Max-Gly RNA gel blotting kit; Austin, TX). RNA gel blots were processed using CDP-*Star* substrate (Roche), and chemiluminescent signals were detected with a Fuji LAS-1000Plus digital imaging system (Fuji Medical Systems, Stamford, CT). The specificity of each riboprobe was determined by blotting of yeast RNA derived from cells ectopically expressing either Cb5-A, -B, -C, or -D. All probes were highly specific, with no cross-hybridization except for probe C, which showed a weak cross-reactivity with Cb5-B RNA (data not shown).

Yeast Strains, Culturing Conditions, and Fatty Acid Analysis

Yeast strains used in this study included BY4742 (matα his3 leu2 lys2 ura3) and a derivative of BY4742 that harbored a disruption of the endogenous Cb5 gene (matα his3 leu2 lys2 ura3 KanMX::cyb5) (strain record number 17382; Invitrogen, Carlsbad, CA). Yeast cells were transformed using a lithium acetate method (Gietz and Woods, 1994), and transformants were maintained at 30°C on synthetic dextrose plates (2% [w/v] dextrose, 0.67% [w/v] yeast nitrogen base without amino acids, and 2% [w/v] agar) containing appropriate auxotrophic supplements. Yeast cells were cultured overnight in liquid synthetic dextrose media at 30°C, then resuspended at $OD_{600} = 0.055$ in synthetic galactose media (2% [w/v] galactose, 0.67% [w/v] yeast nitrogen base without amino acids, and appropriate auxotrophic supplements) and cultured for an additional 24 h. Yeast cells were then harvested and fatty acid composition determined by gas chromatography and flame ionization detection as described previously (Dyer et al., 2002).

Tobacco BY-2 Cell Cultures and Microprojectile Bombardment

Tobacco (*Nicotiana tabacum* cv BY-2) suspension cultures were maintained and prepared for biolistic bombardment as described previously (Banjoko and Trelease, 1995). Transient transformations were performed using 10 μg of plasmid DNA with a biolistic particle delivery system (Bio-Rad Laboratories, Mississauga, Canada) (Lee et al., 1997). For cotransient expression experiments, cells were bombarded with 5 μg of each plasmid DNA. After biolistic bombardment, cells were left for 4 h unless otherwise stated to allow transient expression of the introduced gene(s). BY-2 cells were then processed for immunofluorescence microscopy as described below.

Immunofluorescence Microscopy

BY-2 cells were processed for immunofluorescence microscopy as described by Trelease et al. (1996). Briefly, cells were fixed in formaldehyde, incubated with pectolyase Y-23 (Kyowa Chemical Products, Osaka, Japan), and permeabilized in 0.3% (v/v) Triton X-100. Antibodies and sources were as follows (IgGs were affinity purified using a protein A-Sepharose column): mouse anti-myc antibodies in hybridoma medium (clone 9E10; Princeton University, Monoclonal Antibody Facility, Hybridoma, Princeton, NJ); rabbit anti-E1β (Luethy et al., 1995); rabbit anti-castor bean calreticulin (Coughlan et al., 1997); goat anti-mouse and goat anti-rabbit Alexa Fluor 488 IgGs (Cedar Lane Laboratories, Ontario, Canada); goat anti-rabbit rhodamine red-X IgGs (Jackson ImmunoResearch Laboratories, West Grove, PA). Controls included omitting primary antibodies and mock transformations with vector (pRTL2) alone.

Fluorescent images of cells were acquired using a Zeiss Axioskop 2 MOT epifluorescence microscope (Carl Zeiss, Toronto, Canada) with a Zeiss 63× Plan Apochromat oil-immersion objective. Image captures were performed using a Retiga 1300 charge-coupled device camera (Qimaging, Burnaby, Canada) and Northern Eclipse 5.0 software (Empix Imaging, Mississauga, Canada). Microscopic images of BY-2 cells shown in Figures 2I to 2Q were acquired using a Leica DM RBE microscope with a Leica 100× Plan Apochromat oil-immersion objective and a Leica TCS SP2 scanning head (Leica, Heidelberg, Germany). All fluorescence images of cells shown in individual figures are representative of >50 independent (transient) transformations from at least two independent transformation experiments. Figure compositions were generated using Adobe Photoshop 7.0 (Adobe Systems, San Jose, CA).

Sequence data from this article have been deposited with the EMBL/GenBank data libraries under accession numbers AY578727 for Cb5-A, AY578728 for Cb5-B, AY578729 for Cb5-C, and AY578730 for Cb5-D. Accession numbers for other Cb5s and other proteins described in this study are as follows: Arabidopsis A (NP_180831), Arabidopsis B (NP_200168), Arabidopsis C (AF332415), Borago (U79011), cauliflower (AAA32990), maize A (BQ163226), maize B (BM079024), cotton (BQ403980), Cuscuta (L22209), lettuce (BQ851177), olive A (AJ001370), olive B (CAA04702.1), pineapple (AAM28288), potato A (BM406671.1), potato B (BM112863.1), rice A (BAB63673), rice B (AAK39593.1), tobacco A (X71441), tobacco B (X80008), wheat B (BJ259598.1), and wheat A (BJ218344), yeast (*S. cerevisiae*) (L22494), rat (*Rattus norvegicus*) ER (AF007108), rat outer mitochondrial membrane isoform (NM_030586), rat Vamp2 (AAA42322), rat pOCT (AAA41768), *S. aureus* protein A (AAA26676), and Arabidopsis Tom22 (Q9FNC9).

ACKNOWLEDGMENTS

We thank Sean Coughlan and Jan Mierynk for providing antibodies. We are grateful also to Andrew McCartney for maintaining BY-2 cell cultures, Preetinder Dhanoa for assistance with the construction of plasmids, and other members of our laboratories for their comments during the preparation of the manuscript. This work was supported by the USDA (Current Research Information System project number 6435-41000-083-00D, J.M.D), the Canadian Institute of Heath Research (Grant FRN 10490) to D.W.A., and the Natural Sciences and Engineering Research Council (Grant 217291) to R.T.M. D.W.A. holds a Canada research chair in membrane biogenesis, M.H. is supported by an Ontario graduate scholarship, and R.T.M. is a recipient of an Ontario Premier's Research in Excellence Award.

Received July 14, 2004; accepted August 26, 2004.

REFERENCES

Abell, B.M., Pool, M.R., Schlender, O., Sinning, I., and High, S. (2004). Signal recognition particle mediates post-translational targeting in eukaryotes. EMBO J. **23,** 2755–2764.

Andrews, D.W., Lauffer, L., Walter, P., and Lingappa, V.R. (1989). Evidence for a two-step mechanism involved in assembly of functional signal recognition particle receptor. J. Cell Biol. **108,** 797–810.

Andrews, D.W., Young, J.C., Mirels, L.F., and Czarnota, G.J. (1992). The role of the N region in signal sequence and signal-anchor function. J. Biol. Chem. **267,** 7761–7769.

Bafor, M., Smith, M.A., Jonsson, L., Stobart, K., and Stymne, S. (1993). Biosynthesis of vernoleate (cis-12-epoxyoctadeca-cis-9-enoate) in microsomal preparations from developing endosperm of *Euphorbia lagascae*. Arch. Biochem. Biophys. **303,** 145–151.

Banjoko, A., and Trelease, R.N. (1995). Development and application of an in vivo plant peroxisome import system. Plant Physiol. **107,** 1201–1208.

Beilharz, T., Egan, B., Silver, P.A., Hofmann, K., and Lithgow, T. (2003). Bipartite signals mediate subcellular targeting of tail-anchored membrane proteins in *Saccharomyces cerevisiae*. J. Biol. Chem. **278,** 8219–8223.

Borgese, N., Colombo, S., and Pedrazzini, E. (2003). The tale of tail-anchored proteins: Coming from the cytosol and looking for a membrane. J. Cell Biol. **161,** 1013–1019.

Borgese, N., Gazzoni, I., Barberi, M., Colombo, S., and Pedrazzini, E. (2001). Targeting of a tail-anchored protein to the endoplasmic reticulum and mitochondrial outer membrane by independent but competing pathways. Mol. Biol. Cell **12,** 2482–2496.

Bugos, R.C., Chiang, V.L., Zhang, X.H., Campbell, E.R., Podila, G.K., and Campbell, W.H. (1995). RNA isolation from plant tissues recalcitrant to extraction in guanidine. Biotechniques **19,** 734–737.

Bunkelmann, J.R., and Trelease, R.N. (1996). Ascorbate peroxidase. A prominent membrane protein in oilseed glyoxysomes. Plant Physiol. **110,** 589–598.

Coughlan, S.J., Hastings, C., and Winfrey, R. (1997). Cloning and characterization of the calreticulin gene from *Ricinus communis* L. Plant Mol. Biol. **34,** 897–911.

D'Arrigo, A., Manera, E., Longhi, R., and Borgese, N. (1993). The specific subcellular localization of two isoforms of cytochrome b_5 suggests novel targeting pathways. J. Biol. Chem. **268,** 2802–2808.

Deber, C.M., and Li, S.-C. (1995). Peptides in membranes: Helicity and hydrophobicity. Biopolymers **37,** 295–318.

de Vetten, N., Horst, J.T., van Schaik, H.-P., de Boer, A., Mol, J., and Koes, R. (1999). A cytochrome b_5 is required for full activity of flavanoid 3′,5′-hydroxylase, a cytochrome P450 involved in the formation of blue flower colors. Proc. Natl. Acad. Sci. USA **96,** 778–783.

Dyer, J.M., Chapital, D.C., Kuan, J.-C.W., Mullen, R.T., Turner, C., McKeon, T.A., and Pepperman, A.B. (2002). Molecular analysis of a bifunctional fatty acid conjugase/desaturase from Tung. Implications for the evolution of plant fatty acid diversity. Plant Physiol. **130,** 2027–2038.

Dyer, J.M., and Mullen, R.T. (2001). Immunocytological localization of two plant fatty acid desaturases in the endoplasmic reticulum. FEBS Lett. **494,** 44–47.

Enoch, H.G., Fleming, P.J., and Strittmatter, P. (1979). The binding of cytochrome b_5 to phospholipid vesicles and biological membranes. Effect of orientation on intermembrane transfer and digestion by carboxypeptidase Y. J. Biol. Chem. **254,** 6483–6488.

Falcone, D., and Andrews, D.W. (1991). Both the 5′ untranslated region and the sequences surrounding the start site contribute to efficient initiation of translation *in vitro*. Mol. Cell. Biol. **11,** 2656–2664.

Fritze, C.E., and Anderson, T.R. (2000). Epitope tagging: General method for tracking recombinant proteins. Methods Enzymol. **327,** 3–16.

Gietz, R.D., and Woods, R.A. (1994). High efficiency transformation of yeast. In Molecular Genetics of Yeast: Practical Approaches, J.A. Johnston, ed (New York: Oxford University Press), pp. 121–134.

Gong, F.C., Giddings, T.H., Meehl, J.B., Staehelin, L.A., and Galbraith, D.W. (1996). Z-membranes: Artificial organelles for over-expressing recombinant integral membrane proteins. Proc. Natl. Acad. Sci. USA **93,** 2219–2223.

Horie, C., Suzuki, H., Sakaguchi, M., and Mihara, K. (2002). Characterization of signal that directs C-tail-anchored proteins to mammalian mitochondrial outer membrane. Mol. Biol. Cell **13,** 1615–1625.

Horie, C., Suzuki, H., Sakaguchi, M., and Mihara, K. (2003). Targeting and assembly of mitochondrial tail-anchored protein Tom5 to the TOM complex depend on a signal distinct from that of tail-anchored proteins dispersed in the membrane. J. Biol. Chem. **278,** 41462–41471.

Isenmann, S., Khew-Goodall, Y., Gamble, J., Vadas, M., and Wattenberg, B.W. (1998). A splice-isoform of vesicle-associated membrane protein-1 (VAMP-1) contains a mitochondrial targeting signal. Mol. Biol. Cell **9,** 1649–1660.

Ito, A. (1980). Cytochrome b_5-like hemoprotein of outer mitochondrial membrane, OM cytochrome b: II. Contribution of OM cytochrome b to rotenone-insensitive NADH-cytochrome c reductase activity. J. Biochem. **87,** 73–80.

Ito, A., Hayashi, S., and Yoshida, T. (1981). Participation of a cytochrome b_5-like hemoprotein of outer mitochondrial membrane (OM cytochrome b) in NADH-semidehydroascorbic acid reductase activity of rat liver. Biochem. Biophys. Res. Commun. **101,** 591–598.

Janiak, F., Glover, J.R., Leber, B., Rachubinski, R.A., and Andrews, D.W. (1994a). Targeting of passenger proteins to multiple intracellular membranes. Biochem. J. **300,** 191–199.

Janiak, F., Leber, B., and Andrews, D.W. (1994b). Assembly of Bcl-2 into microsomal and outer mitochondrial membranes. J. Biol. Chem. **269,** 9842–9849.

Kaufmann, T., Schlipf, S., Sanz, J., Neubert, K., Stein, R., and Borner, C. (2003). Characterization of the signal that directs Bcl-x(L), but not Bcl-2, to the mitochondrial outer membrane. J. Cell Biol. **160,** 53–64.

Kim, P.K., Hollerbach, C., Trimble, W.S., Leber, B., and Andrews, D.W. (1999). Identification of the endoplasmic reticulum targeting signal in vesicle-associated membrane proteins. J. Biol. Chem. **74,** 36876–36882.

Kim, P.K., Janiak-Spens, F., Trimble, W.S., Leber, B., and Andrews, D.W. (1997). Evidence for multiple mechanisms for membrane binding and integration via carboxyl-terminal insertion sequences. Biochemistry **36,** 8873–8882.

Kozak, M. (1999). Initiation of translation in prokaryotes and eukaryotes. Gene **234,** 187–208.

Kuroda, R., Ikenoue, T., Honsho, M., Tsujimoto, S., Mitoma, J.Y., and Ito, A. (1998). Charged amino acids at the carboxyl-terminal portions determine the intracellular locations of two isoforms of cytochrome b_5. J. Biol. Chem. **273,** 31097–31102.

Kutay, U., Hartmann, E., and Rapoport, T.A. (1993). A class of membrane proteins with a C-terminal anchor. Trends Cell Biol. **3,** 72–75.

Kyte, J., and Doolittle, R.F. (1982). A simple method for displaying the hydropathic character of a protein. J. Mol. Biol. **157,** 105–132.

Lederer, F., Ghrir, R., Guiard, B., Cortial, S., and Ito, A. (1983). Two homologous cytochromes b_5 in a single cell. Eur. J. Biochem. **132,** 95–102.

Lee, M.S., Mullen, R.T., and Trelease, R.N. (1997). Oilseed isocitrate lyases lacking their essential type 1 peroxisomal targeting signal are piggybacked to glyoxysomes. Plant Cell **9,** 185–197.

Lisenbee, C.S., Karnik, S.K., and Trelease, R.N. (2003). Overexpression and mislocalization of a tail-anchored GFP redefines the identity of peroxisomal ER. Traffic **4,** 491–501.

Luethy, M.H., David, N.R., Elthon, T.E., Mierynk, J.A., and Randall, D.D. (1995). Characterization of a monoclonal antibody directed against the E1α subunit of plant pyruvate dehydrogenase. J. Plant Physiol. **145,** 442–449.

Macasev, D., Newbigin, E., Whelan, J., and Lithgow, T. (2000). How do plant mitochondria avoid importing chloroplast proteins? Components of the import apparatus Tom20 and Tom22 from *Arabidopsis* differ from their fungal counterparts. Plant Physiol. **123,** 811–816.

Mathews, F.S. (1985). The structure, function and evolution of cytochromes. Prog. Biophys. Mol. Biol. **45,** 1–56.

McCartney, A.W., Dyer, J.M., Dhanoa, P.K., Kim, P.K., Andrews, D.W., McNew, J.A., and Mullen, R.T. (2004). Membrane-bound fatty acid desaturases are inserted co-translationally into the ER and contain different ER retrieval motifs at their carboxy termini. Plant J. **37,** 156–173.

Mitoma, J., and Ito, A. (1992). The carboxy-terminal 10 amino acid residues of cytochrome b_5 are necessary for its targeting to the endoplasmic reticulum. EMBO J. **11,** 4197–4203.

Mullen, R.T., Lisenbee, C.S., Flynn, C.R., and Trelease, R.N. (2001). Stable and transient expression of chimeric peroxisomal membrane proteins induces an independent ''zippering'' of peroxisomes and an endoplasmic reticulum subdomain. Planta **213,** 849–863.

Mullen, R.T., Lisenbee, C.S., Miernyk, J.A., and Trelease, R.N. (1999). Peroxisomal membrane ascorbate peroxidase is sorted to a membranous network that resembles a subdomain of the endoplasmic reticulum. Plant Cell **11,** 2167–2185.

Mullen, R.T., and Trelease, R.N. (2000). The sorting signals for peroxisomal membrane-bound ascorbate peroxidase are within its C-terminal tail. J. Biol. Chem. **275,** 16337–16344.

Napier, J.A., Michaelson, L.V., and Sayanova, O. (2003). The role of cytochrome b_5 fusion desaturases in the synthesis of polyunsaturated fatty acids. Prostaglandins Leukot. Essent. Fatty Acids **68,** 135–143.

Ohlrogge, L., and Browse, J. (1995). Lipid biosynthesis. Plant Cell **7,** 957–970.

Pedrazzini, E., Villa, A., Longhi, R., Bulbarelli, A., and Borgese, N. (2001). Mechanism of residence of cytochrome b(5), a tail-anchored protein, in the endoplasmic reticulum. J. Cell Biol. **148,** 899–914.

Perara, E., and Lingappa, V.R. (1985). A former amino terminal signal sequence engineered to an internal location directs translocation of both flanking protein domains. J. Cell Biol. **101,** 2292–2301.

Petrini, G.A., Altabe, S.G., and Uttaro, A.D. (2004). *Trypanosoma brucei* oleate desaturase may use a cytochrome b_5-like domain in another desaturase as an electron donor. Eur. J. Biochem. **271,** 1079–1086.

Pratelli, R., Sutter, J.U., and Blatt, M.R. (2004). A new catch in the SNARE. Trends Plant Sci. **9,** 187–195.

Remacle, J. (1978). Binding of cytochrome b_5 to membranes of isolated subcellular organelles from rat liver. J. Cell Biol. **79,** 291–313.

Sambrook, J., Fritsch, E.F., and Maniatis, T. (1989). Molecular Cloning: A Laboratory Manual, 2nd ed. (Cold Spring Harbor, NY: Cold Spring Harbor Laboratory Press).

Sanderfoot, A.A., Assaad, F.F., and Raikhel, N.V. (2000). The *Arabidopsis* genome. An abundance of soluble N-ethylmaleimide-sensitive factor adaptor protein receptors. Plant Physiol. **124,** 1558–1569.

Schägger, H., and von Jagow, G. (1987). Tricine-sodium dodecyl sulfate-polyacrylamide gel electrophoresis for the separation of proteins in the range from 1 to 100 kDa. Anal. Biochem. **166,** 368–379.

Schenkman, J.B., and Jansson, I. (2003). The many roles of cytochrome b_5. Pharmacol. Ther. **97,** 139–152.

Seedorf, M., Waegemann, K., and Soll, J. (1995). A constituent of the chloroplast import complex represents a new type of GTP-binding protein. Plant J. **7,** 401–411.

Smith, M.A., Cross, A.R., Jones, O.T., Griffiths, W.T., Stymne, S., and Stobart, K. (1990). Electron-transport components of the 1-acyl-2-oleoyl-sn-glycerol-3-phosphocholine delta 12-desaturase (delta 12-desaturase) in microsomal preparations from developing safflower (*Carthamus tinctorius* L.) cotyledons. Biochem. J. **272,** 23–29.

Smith, M.A., Jonsson, L., Stymne, S., and Stobart, K. (1992). Evidence for cytochrome b_5 as an electron donor in ricinoleic acid biosynthesis in microsomal preparations from developing castor bean (*Ricinus communis* L.). Biochem. J. **287,** 141–144.

Smith, M.A., Stobart, A.K., Shewry, P.R., and Napier, J.A. (1994). Tobacco cytochrome b_5: cDNA isolation, expression analysis and in vitro protein targeting. Plant Mol. Biol. **25,** 527–537.

Snapp, E.L., Hegde, R.S., Francolini, M., Lombardo, F., Colombo, S., Pedrazzini, E., Borgese, N., and Lippincott-Schwartz, J. (2003). Formation of stacked ER cisternae by low affinity protein interactions. J. Cell Biol. **163,** 257–269.

Sonntag, N.O.V. (1979). Composition and characteristics of individual fats and oils. In Bailey's Industrial Oil and Fat Products, D. Swern, ed (New York: John Wiley & Sons), pp. 289–477.

Surpin, M., and Raikhel, N. (2004). Traffic jams affect plant development and signal transduction. Nat. Rev. Mol. Cell Biol. **5,** 100–109.

Takagaki, Y., Radhakrishnan, R., Gupta, C., and Khorana, H. (1983a). The membrane-embedded segment of cytochrome b_5 as studied by cross-linking with photoactivable phospholipids. I. The transferable form. J. Biol. Chem. **258,** 9128–9135.

Takagaki, Y., Radhakrishnan, R., Wirtz, K., and Khorana, H. (1983b). The membrane-embedded segment of cytochrome b_5 as studied by cross-linking with photoactivable phospholipids. II. The nontransferable form. J. Biol. Chem. **258,** 9136–9142.

Tanaka, S., Kinoshita, J.Y., Kuroda, R., and Ito, A. (2003). Integration of cytochrome b5 into endoplasmic reticulum membrane: Participation of carboxy-terminal portion of the transmembrane domain. J. Biochem. **133,** 247–251.

Trelease, R.N., Xie, W., Lee, M.S., and Mullen, R.T. (1996). Rat liver catalase is sorted to peroxisomes by its C-terminal tripeptide Ala-Asn-Leu, not by the internal Ser-Lys-Leu motif. Eur. J. Cell Biol. **71,** 248–258.

Vergeres, G., Yen, T.S., Aggeler, J., Lausier, J., and Waskell, L. (1993). A model system for studying membrane biogenesis. Overexpression of cytochrome b5 in yeast results in marked proliferation of the intracellular membrane. J. Cell Sci. **106,** 249–259.

Walter, P., and Blobel, G. (1983). Preparation of microsomal membranes for cotranslational protein translocation. Methods Enzymol. **96,** 84–93.

Wattenberg, B., and Lithgow, T. (2001). Targeting of C-terminal (tail)-anchored proteins: Understanding how cytoplasmic activities are anchored to intracellular membranes. Traffic **2,** 66–71.

Werhahn, W., Niemeyer, A., Jansch, L., Kruft, V., Schmitz, U.K., and Braun, H. (2001). Purification and characterization of the preprotein translocase of the outer mitochondrial membrane from *Arabidopsis*. Identification of multiple forms of TOM20. Plant Physiol. **125,** 943–954.

Whitley, P., Grahn, E., Kutay, U., Rapoport, T.A., and von Heijne, G. (1996). A 12-residue-long polyleucine tail is sufficient to anchor synaptobrevin to the endoplasmic reticulum membrane. J. Biol. Chem. **271,** 7583–7586.

Zhao, J., Onduka, T., Kinoshita, J.Y., Honsho, M., Kinoshita, T., Shimazaki, K., and Ito, A. (2003). Dual subcellular distribution of cytochrome b5 in plant, cauliflower, cells. J. Biochem. **133,** 115–121.